Reverse Engineering Report

Cyril W. Moran
University of Florida, Gainesville, Florida, 32608

UF ID: 11834191
Word Count:

Submission Date: June 3rd, 2022

Table of Contents

I. Introduction

This report aims to reverse engineer a Supertek® 50ml acrylic burette. The purpose of this burette is to dispense and measure liquids and is especially used in chemistry applications such as titration. This project conducts an in-depth analysis and deconstruction of a burette. The resulting analyses will be used to develop an understanding of the function of the product and its comprising parts, to model the product in Solidworks, to understand the fundamental engineering principles and physics that govern the product, and to construct a dimensional analysis of the burette highlighting the tolerances that accompany each part and functional surface.

In order to reconstruct and reproduce the burette it is first deconstructed, and all the critical dimensions are measured using calipers. Once the burette is fully disassembled a CAD model in Solidworks will be modeled to represent it and to develop drawings for the parts and assemblies. The materials of each part are then determined experimentally by performing certain tests (such as setting part on fire) and comparing results to a database of known materials and properties.

Then an analysis on the engineering principles surrounding the function of the burette is conducted and reported. The tolerances of each part and sub-assembly are determined using tolerance loops. The goal of this project is to successfully reverse engineer the burette and gain an understanding of the engineering principles and tolerances that went into designing this product.

II. Gantt Chart

A Gantt chart was produced for the Reverse Engineering Report (RER) to display the different tasks and the estimated allocation of time for each task in Fig.(1). Each task follows the completion of the previous task, and 3 different milestones show when considerable parts of the project are expected to be completed. Additionally, each different task requires resources that are either human or physical that were utilized to complete this project.

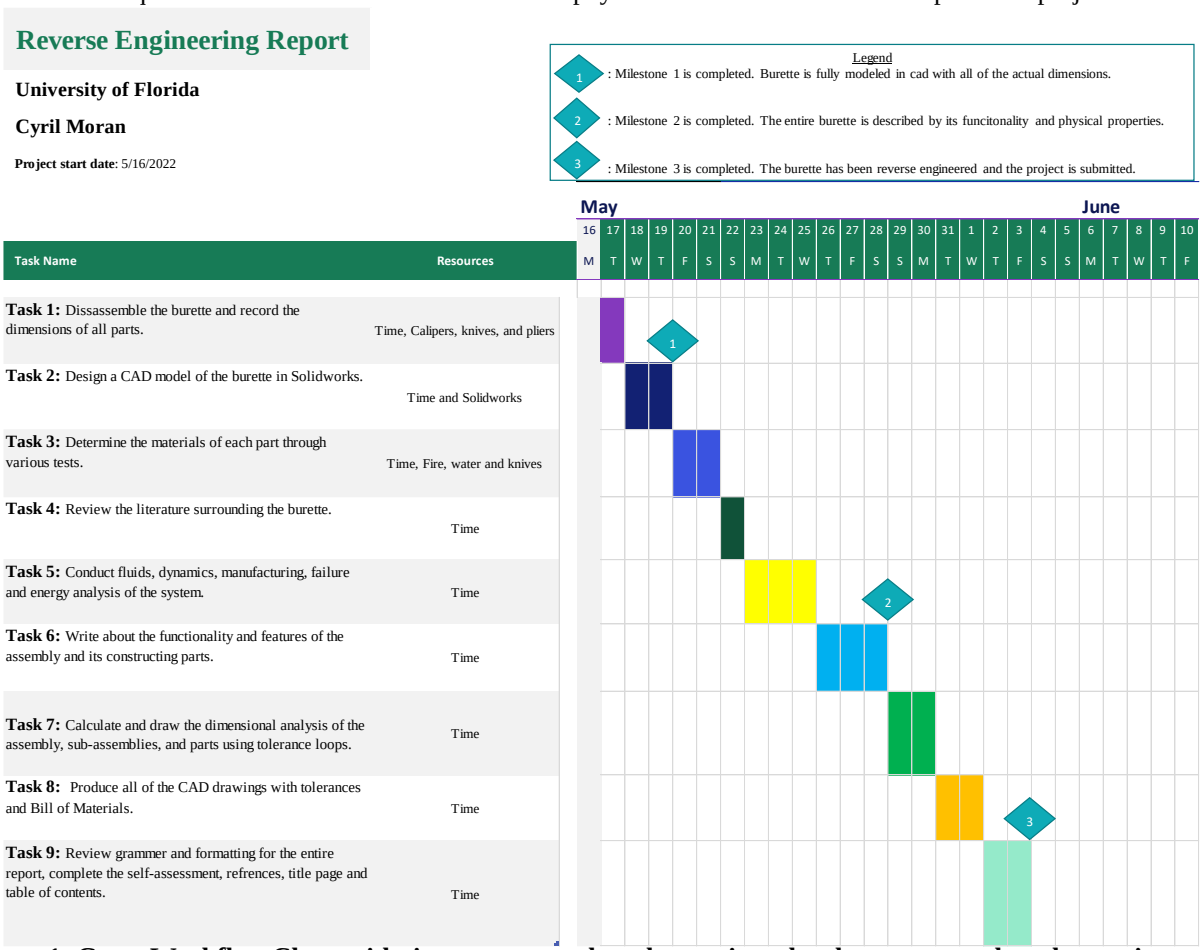

Figure 1: Gantt Workflow Chart with time represented on the x-axis and tasks represented on the y-axis

The actual workflow and the produced Gantt chart had substantial differences in terms of the time allocated to different tasks. The initial idea for the development of this project was to dedicate days to different topics and depending on the estimated intensity of a topic, time was allocated respectively. The realization hit me about halfway through the project on May 25th that each of these topics is very intertwined and it will be difficult to fully complete a section before completing it fully. The development of the burette in CAD and recording of all of the measurements of the artifact was completed according to schedule. After the discrete parts of the project were completed all of the other parts which included more creativity and analysis took substantially longer than originally planned.

I also didn't take into account the fact that there would be some topics and tasks that I wouldn't fully understand so it would take me longer to conduct the proper research and utilize all the resources that were given to me. This first occurred when I was supposed to write the literature review and I wasn't able to find any similar patents or standards and I just pushed it off until later. This was the first major deviation from the Gantt chart. The second deviation was the engineering analysis task that I assumed would only take 3 days. I have never conducted creative and intense analyses like this before on a generic product, so it heavily overestimated my capabilities. The actual time that these engineering analyses were completed was from May 23-29th which is 4 days over my original plan. While this didn't go according to my original workflow it didn't put me behind on work since I was working on other tasks in tandem with these analyses. I was conducting some of the tolerance loop analyses and writing some of the literature review as I received more information about the burette as I conducted each analysis.

The Gantt chart was followed intensely for the first 5 days and then it didn't predict the workflow to any capacity. In order to develop Gantt charts in the future that more accurately represent my estimated time allocation, I need to consider both the quantity and quality of the work that is required. Taking time to sit down and write down a preliminary analysis of the project and determine my weak and strong points in which I can accurately predict the estimated time. This time allocation includes background research for topics that I am not familiar with and reaching out to my superiors and asking them for some insight and guidance on certain tasks.

This Gantt chart was useful in the beginning to develop a mental schedule of what tasks needed to be completed and the logical progression of tasks. This chart will help with the development of future Gantt charts by illustrating what tasks and types of tasks were most accurately represented by the time it would take to complete them. Utilizing all of this information will improve future Gantt charts and project management.

III. Product Overview

A. Literature Review

Titration has been a critical tool used in various aspects of chemical analysis since the 18th century. It measures the volume of a reagent required to elicit a reaction of its mixture with another. This is used to determine the acidity or basicity of an analyte, the identity of the analyte, and many more properties. The first titration was performed in 1729 by Claude Geoffroy who determined the acidity of various kinds of vinegar [9]. This demonstrated to the world that this technique could be used to determine the quality of common things that we eat and to quantify their safety. The first titration paraphernalia used was named an alkalimeter which consisted of a graduated tube with two pipes for the titrate and the analyte. The mixing of the analyte and titrate took place in the graduated cylinder and the overall volume was recorded [9]. This resulted in a lot of uncertainty in the measured results due to the leaking of the pipettes and the large measurement readings on the graduated cylinder which had 1cm increments.

As time passed there were new and innovative titration techniques that become integrated into chemistry. New techniques such as precipitation titration to determine the purity of silver, and iodometric titration to determine what substances oxidized iodine from potassium iodide. The modern burette design is based on the design from Etienne Henry in 1846 [9]. This tap burette consisted of a long-graduated cylinder that deposited a controlled amount of liquid into a cone-shaped reservoir that contained a known solution of a known volume. This burette led to the invention of the modern burette and was significantly improved by developing plastic burette bodies, liquid-tight stopcocks and plugs, and more precise nozzles [9].

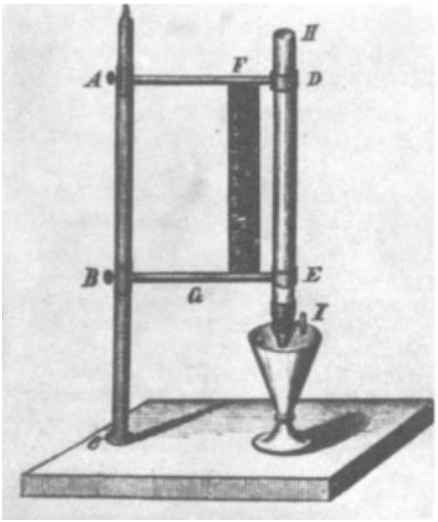

Figure 2: Etienne Henry's tap burette which was used to determine concentrations of different drugs in 1846. []

This burette that this project investigates is based on this model of burettes. The conceptual design has the same foundation as Henry's tap burette. The modern burette has been modified over the years to become increasingly accurate, precise, user-friendly, cheaper, and durable. The invention of the stopcock and the plug allowed for the majority of these improvements to occur. The stopcock allowed for the graduated cylinder portion of the burette to remain leak-free and be able to control when and how much liquid was dispensed. This stopcock provided the burette with a smooth and consistent pathway for the liquid to leave the burette and enter the reservoir. The first design of the stopcock that led to the improvement of the burette was invented by J. Dunbeck and W. Hanf in 1962 [8].

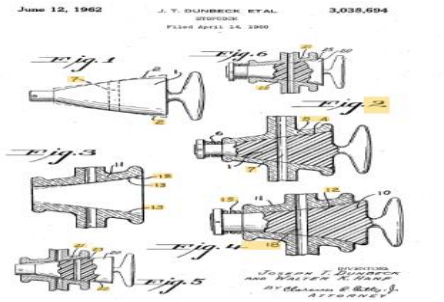

Figure 3: Stopcock to prevent leakage [8].

The design quality of this stopcock was that it aimed to increase the pressure the plug imposed on the stopcock wall to prevent liquid to spill. This is the same design as the burette this paper is investigating. The burette this paper is observing has a stopcock and a plug which form an interference fit to impose a pressure that prevents the leakage of water that's stored inside of the burette housing.

The transition of burette bodies from glass to plastic occurred rather recently with one of the popular ones being developed in 1962. Due to plastics' higher ultimate stress and fracture point made them more durable. For accidents that are unavoidable in the lab such as dropping or hitting the burette, the glass burette would have a much greater chance of breaking. This transition to plastic allowed for the burette to have a longer fatigue life and it reduced the costs of buying a burette. The manufacturing methods and materials used to make glass burettes are much more expensive than making plastics with injection molding. These modern burettes can be made for much cheaper and they can be produced in larger volumes increasing the availability of burettes to everyone interested in science.

The modern burette can perform a variety of different titration methods and can do so with 0.5mL accuracy. These advancements made over the centuries have become mainstream in every single company that produces products. Ranging from the food suppliers testing the acidic content of their products to schools that use titration to teach it to the upcoming generations, these modern burettes are used in everyday life and are powerful tools.

B. Product Functionality

The functionality of the product was determined and analyzed. The burette has many distinct functions that it achieves through various mechanisms.

One of the main functions is the burettes' ability to store and measure a static or dynamic volume of liquid (50 ml max). The burette housing has graduation marks approximately 1 mm apart and can measure volumes of liquid up to a 0.5 ml accuracy. Each graduation mark represents 1 ml of liquid present in the burette housing.

A related function of the burette is its ability to dispense liquid at a controlled and constant rate. What enables this feature is the stopcock plug. The stopcock plug has a greater outer diameter than the stopcock housing which results in pressure being applied on the housing walls. This pressure exceeds the hydrostatic pressure of the liquid in the burette which results in no leakage. The plug has a hole of a diameter magnitudes smaller than the outer diameter which can be rotated by rotating the plug in the stopcock housing. This hole can then be aligned with the hole of the stopcock body, or it can be in contact with the wall. The aligning of the plug allows the liquid to flow from the burette housing out of the nozzle which will be a constant volumetric flow rate due to gravity and the cross-sectional area of the outlet.

The 3 O-rings secured into the grooves of the stopcock housing allow the burette to be leakproof. The O-rings accomplish this by being elastically deformed by the installation of the burette housing and exerting pressure onto it. This pressure is caused by the O-ring's and burette housing's contact area and the force from the O-ring deformation. The pressure that is exerted by the O-rings onto the burette housing is higher than the hydrostatic pressure of the liquid in the burette which prevents liquid to leak. The 3 O-rings are installed above each other as a safety measure to ensure that the liquid won't leak if an O-ring fails. The O-rings also allow the burette to be disassembled with no specific tools in order to clean or replace the burette housing. The burette housing can be removed by pulling on the burette housing with enough force to overcome the friction between the O-ring and the burette walls and to deform the O-ring until it complies. The O-rings material properties (elasticity) and the fact that the burette/stopcock assembly isn't one piece enable the burette housing to be removed.

The O-ring secured into the groove of the stopcock plug allows for the removal of the plug from the stopcock housing and restricts lateral movement of the plug. The plug can be removed from the stopcock body by pulling on it with enough force to deform the O-ring enough for it to be removed. Unintentional lateral movement is also reduced due to the amount of force that needs to be applied to the plug to overcome the O-ring deformation being larger than the accidental forces the plug will endure. The elasticity and deformation properties of the O-ring make the subassembly separable and resistant to lateral movement.

The burettes' ability to precisely dispense varying volumes of liquid is because of the nozzle. The nozzle has a variable cross-sectional area that decreases along with the flow of the fluid. This allows for less uncertainty in the volumetric flow rate of the liquid and for smaller amounts of volume to be dispensed (important for titration). The converging cross-sectional area of the nozzle allows for this reduction in liquid flow which results in less uncertainty and more precise dispensed volumes of liquids.

The stopcock housing allows for the transition of fluid flow from the burette housing to the nozzle outlet. Once the stopcock plug is turned so the hole isn't in contact with the wall of the stopcock housing, the liquid inside of the burette flows through the hole, into the nozzle, and out of the nozzle's outlet. This is because of the pressure gradient between the atmosphere and the volume of liquid inside of the burette and since the stopcock nozzle has a thru-hole the liquid can flow. Additionally, the stopcock housing and nozzle interface allow the liquid to flow from the stopcock to the nozzle.

The flow of liquid can easily be enabled or stopped with the handle. The handle is inserted inside of the plug, and it rotates which rotates the hole to either be in contact with the wall or not. A torque applied to the handle will enable the rotation of the plug if it exceeds the frictional torque between the plug and the stopcock wall. The length of the handle and the interference fit of the plug/stopcock assembly allow for this to happen.

The flow of liquid is perpendicular to the earth's surface, clamped to prevent lateral movement during flow, and raised off the ground to be put inside of a reservoir. A retort stand has a heavy base and vertical rod where it clamps onto the burette housing which restricts the flow of liquid to the vertical direction, and which ensures the maximum hydrostatic pressure value. The vertical rod, heavy base, and clamp make it so the burette is off the ground and vertical so the flow of liquid can be accurate and consistent.

C. Manufacturing and Assembly

The assembly methods for the burette were determined using both theoretical and empirical analyses. The theoretical analysis that was used for the determination of assembly time and assembly steps was the Boothroyd & Dewhurst Technique.

This technique utilizes two different charts of data to sum all of the total times each assembly step takes to develop a total assembly time. The two different assembly types are handling and inserting. To determine how much time a specific step will take there were a few characteristics that had to be determined for each assembly step. The first step was determining whether or not this was a handling of a component or an insertion of components. This step determined which chart was used to determine the time. If it was a handling step, then 4 different quantities were measured and then used to determine that step's specific handling/insertion code which corresponds to a time in seconds. These quantities are as follows: Alpha Symmetry (α), Beta Symmetry (β), Thickness (t), Size (s) [10]. The alpha symmetry angle was determined by the number of degrees the part needs to rotate about the axis perpendicular to insertion to repeat the same orientation from the start. The beta symmetry angle was determined by the number of degrees the part needed to rotate about the insertion axis before it repeated its initial orientation. The thickness is the dimension of the smallest side. Size is the dimension of the largest side. Every single component in the handling steps for the assembly was analyzed to determine these quantities in order to determine the time required to complete that step. The handling step also consists of 3 different charts which utilize these same variables to determine the time to complete the process, but they differ by the difficulty/extent of handing for each of these parts (one hand, two hands, tools).

The other assembly category used in the Boothroyd & Dewhurst Chart is insertion. When the assembly step consisted of inserting/combining two different components together it was an insertion. The three different insertion types are: Part Added but Not Secure, Part Secured Immediately, and Separate Operation. Each of these types of insertions have several factors used to determine the step time. Every single insertion process was analyzed to determine the insertion type and the corresponding characteristics of the process to determine the time.

The estimated assembly time calculated for this burette assembly using the Boothroyd & Dewhurst Chart is shown below in Table (1).

Table 1: Theoretical Assembly Time

Step #	H / I Process	α Angle	β Angle	α + β Sum	H / I Code	Process Time (s)	Justification
1	H	360	0	360	(1,0)	1.5	
2	H	360	0	360	(1,0)	1.5	Thickness value was taken 10ml from the end that was picked up
3	I	N/A	N/A	0	(3,0)	2	
4	H	360	0	360	(1,0)	1.5	Thickness value was taken from smaller OD
5	I	N/A	N/A	0	(3,4)	6	
6	H	180	0	180	(0,0)	1.13	Thickness taken from tapered end.
7	I	N/A	N/A	0	(3,4)	6	
8	H	180	0	180	(0,3)	1.69	Thickness is height of O-Ring and size is OD
9	I	N/A	N/A	0	(4,4)	8.5	
10	H	180	0	180	(0,3)	1.69	
11	I	N/A	N/A	0	(3,4)	6	
12	H	180	0	180	(0,3)	1.69	
13	I	N/A	N/A	0	(0,9)	7.5	
14	H	180	0	180	(0,3)	1.69	
15	I	N/A	N/A	0	(1,9)	10	
16	H	360	0	360	(1,0)	1.5	
17	I	N/A	N/A	0	(3,4)	6	
18	I	N/A	N/A	0	(9,8)	9	
					Total Time	74.89	

Using this method to determine the assembly time, it was found that it would take 74.89 seconds to completely assemble each component of this burette into the complete assembly. There was a total of 18 different steps that made up the assembly process.

A real-world analysis was also conducted to compare the differences in calculated assembly times. From a sample size of 55 different assemblies the average assembly time was 76.83 seconds with a standard deviation of 51.32 seconds. Analyzing the data, it was found that 13.32% of the values will lie within 95% of the range of possible population times. This is unreliable and illustrates immense uncertainty in the data collected. A reason for this uncertainty is due to several factors such as person to person assembling capabilities and the lack of assembly experience. As someone assembles more burettes, they will develop new methods that reduce the total assembly time. Data was taken from 10 consecutive assemblies to illustrate this learning curve. Figure (2) below graphs the relationship between consecutive assemblies and assembly time.

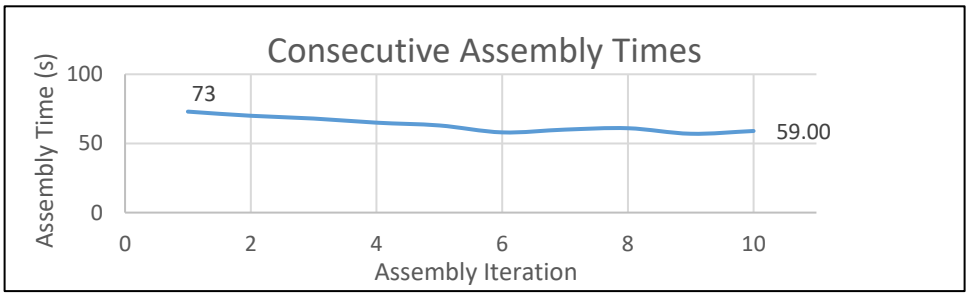

Figure 4: Assembly Time vs. Consecutive Assemblies

There are a variety of several factors that affect assembly time, and it can be seen how much assembly time reduces when person assembling the devices becomes more familiar with the processes. From this it can be concluded that the most reliable assembly time for this burette is the theoretical one using the Boothroyd & Dewhurst Technique. This is an industry standard technique for manufacturing times and has substantially more data supporting its assertions that the amount of data our report generated. It can be concluded that the total assembly time for the burette is 74.89 seconds.

Below are detailed images that illustrate the steps in the assembly process from start to finish.

Steps 1-2: Picking up stopcock body and nozzle.

Step 3: Inserting nozzle into stopcock body.

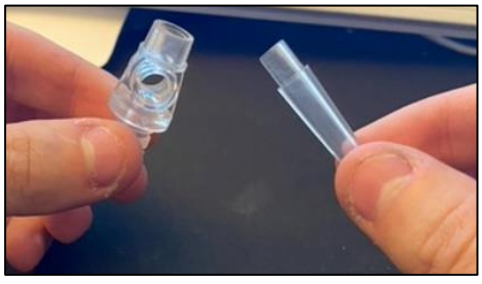

Step 4: Picking up plug.

Step 5: Inserting plug into sub-assembly.

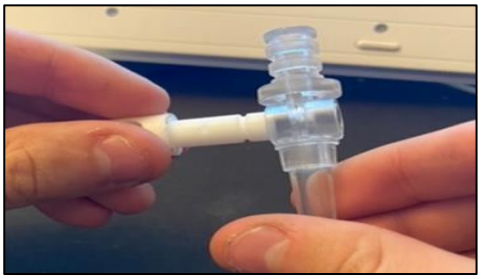

Step 6: Picking up the handle.

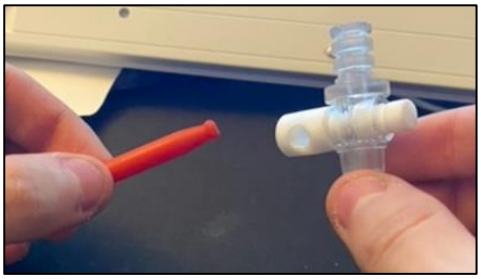

Step 7: Inserting handle into sub-assembly.

Step 8: Picking up small O-ring.

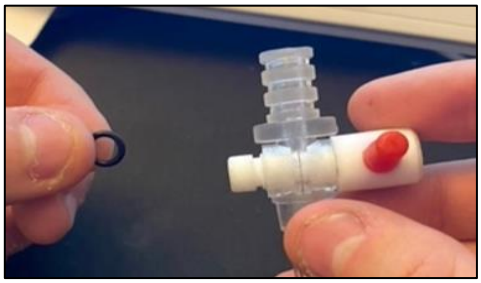

Step 9: Inserting O-ring into plug groove.

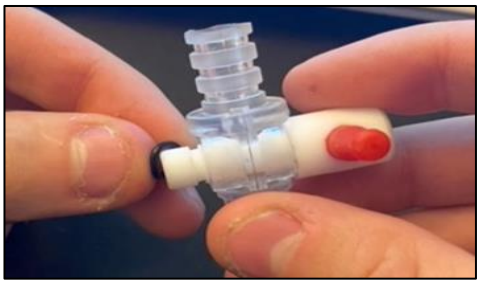

Step 10: Picking up top O-ring.

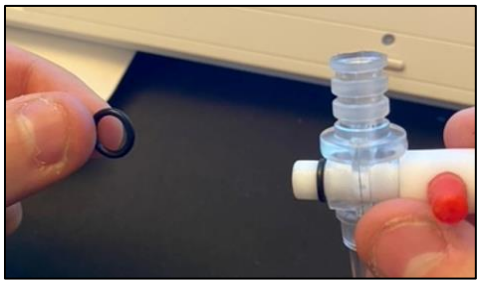

Step 11: Inserting top O-ring into top stopcock groove.

Step 12: Picking up middle O-ring.

Step 13: Inserting middle O-ring into middle stopcock groove.

Step 14: Picking up bottom O-ring.

Step 15: Inserting bottom O-ring into bottom stopcock groove.

Step 16: Picking up burette housing

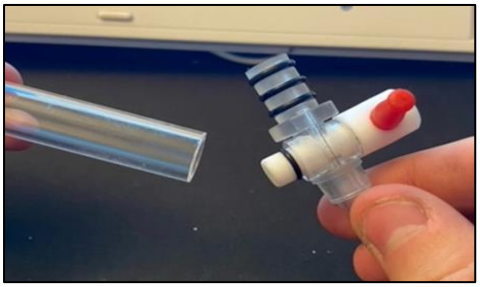

Step 17: Insert stopcock sub-assembly into burette housing.

Step 18: Check assembly for proper O-ring installation.

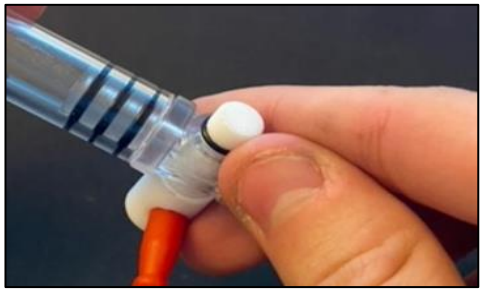

D. Materials

Every single component of the burette assembly underwent a material determination process. The list of the components and their determined materials are as follows:

1. **Burette Housing**- Acrylic
2. **Stopcock Body**- Polyethylene (PE)
3. **Nozzle**- Polypropylene (PP)
4. **Handle**- Polyethylene (PE)
5. **Plug**- Polytetrafluorethylene (PTFE)
6. **O-Rings**- Styrene

The process for the determination of materials consisted of subjecting each component of the burette assembly to different tests and then using the Plastics and Elastomers Identification Chart shown below in Fig.(2) to determine the identity of the plastic through process of elimination.

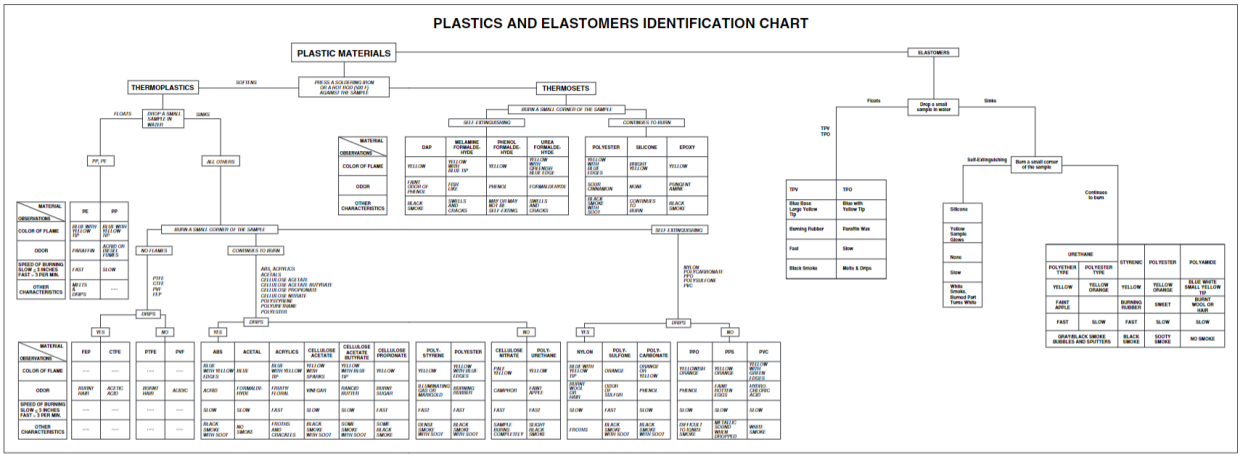

Figure 5: Plastics and Elastomers Identification Chart [11]

The first material that was identified was the handle. The first test was to press a soldering iron against the sample and see if it softens or if it doesn't. From the following picture the handle was observed to soften in Fig.(6).

Figure 6: Soldering iron touching handle [12]

Figure 7: Handle on fire

This test determined that this was a thermoplastic. To determine the type of thermoplastic the next test was to drop the sample in water and observe its buoyancy properties (if it floats or not). The specimen floated in the water which narrowed it down to either polyethylene or polypropylene. The final test was lighting the specimen on fire and observing a variety of different possible characteristics. The 3 dissimilar characteristics between PE and PP are the odor, speed of burning, and melting/dripping. Figure (7) above illustrates that the handle melted and dripped when it was lit on fire. These tests reveal the identity of the material for the handle is PE.

The second material that was identified was the nozzle. The first test was to press a soldering iron against the sample body to observe softening or not. From Fig.(8) below the nozzle was observed softening. This test determined that it was also a thermoplastic, and the next test was to see if it floated in water. The nozzle floated in the water which narrowed it down to either PE or PP plastic. The nozzle was then lit on fire to determine its actual identity. Fig.(6) below shows the nozzle on fire where the determining characteristic were the diesel fumes it produced. This process determined the material identity of the nozzle to be PP.

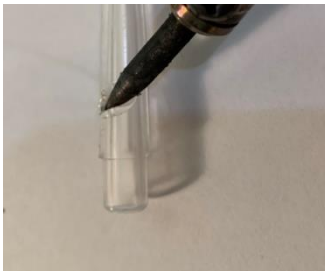

Figure 8: Soldering iron touching handle [8]

Figure 9: Nozzle Burning

The third material that was identified was the stopcock body. The soldering iron test was conducted first and from the picture below it was observed that it softened in Fig.(10). The next test was to drop it in water to see if it floated. The stopcock floated in the water which narrowed it down to PE or PP as possible materials. The stopcock was lit on fire and Fig.(11) below shows the observations. The stopcock melted and dripped when it was lit on fire which results in the stopcock identity in being PE.

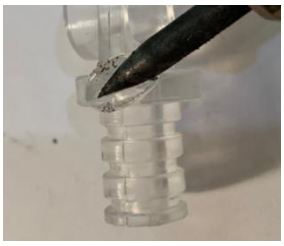

Figure 10: Soldering iron touching stopcock [14]

Figure 11: Stopcock on fire

The fourth material that was identified was the O-ring. The first test was to drop the specimen in water, and it sunk. The second test conducted was lighting it on fire and observing whether the flame was self-extinguishing or continually burning. The O-ring was observed to be continually burning and is represented by the picture below in Fig.(12). The differentiating characteristics that were observed was that it burned fast and that there was black smoke. These two characteristics resulted in the only possible material identity of the O-rings to be Styrene.

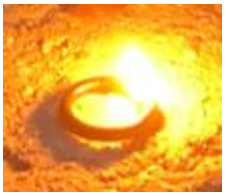

Figure 12: O-ring on fire

The fifth material that was identified was the plug. Before tests were conducted on this material the 2020 Supertek® Catalog was referenced and it stated that the plug was comprised of PTFE [16]. Due to the dangers of burning PTFE can cause to human lungs the plug wasn't tested using the same deterministic processes as the other components and the material was assumed to be PTFE.

The sixth and final material that was identified was the burette housing. The first test that was conducted was pressing a soldering iron against the burette housing body. The burette housing was observed to soften and is represented by the picture below. The next test was to drop the burette housing in water and observe if it floated or not. The burette sunk which leads to the final test of burning the burette housing. The burette housing was observed to continually burn and drip when it was ignited. The burette housing frothed and crackled in the flames when it was on fire which narrowed the material identity of the burette housing down to acrylics. This result was verified by the 2020 Supertek® Catalog which states on page 15 that the burette artifact is made of an acrylic body [16].

Figure 13: Soldering iron on burette housing [15]

All of the materials that were identified were found using the same process of elimination and using the same identification chart. Every material will differ in manufacturing methods because of different material types, sizes, and desired material properties. The most common material was polypropylene in the burette assembly. The most material by volume was acrylic, which comprised the burette housing.

E. Functional Analysis

The aim of performing these functional analyses on the burette assembly and subassemblies is to quantitatively determine and understand the physics that guided these design decisions. Every single component of this burette is subjected to the laws of physics and to be able to develop a design standard to satisfy all of the physical requirements is what this section accomplishes. There are 5 different types of analyses that this report focuses on and those include: Dynamics, Finite Element Analysis (FEA), Energy, Machine Design, and Fluid Mechanics. This is not an extensive list, but this is the most relevant engineering principles that govern the burette.

1. Dynamics Analysis

2. Kinematics of the Handle and Plug

This burette assembly has various dynamical devices that govern its motion. One of the main ones is the minimum torque that can be applied to the handle to facilitate easy turning of the plug. The torque applied to the handle can be represented by the following equation:

$$2T = F \cdot d \tag{1}$$

Torque is multiplied by 2 since there are two fingers torquing the handle at opposite ends but in the same direction. There is also resistance to the applied torque in the form of frictional torque that is opposing the motion to the applied torque and is determine by the properties of the plug and interference fit.

$$T_f = \mu \cdot F_p \cdot r_p$$

F is the applied force, d is the distance of the moment arm, r_p is the radius of the plug, T_f is the frictional torque, F_p is the force the plug exerts onto the stopcock, and T is the resulting torque. The moment arm is defined below where L_h is the length of the handle, and d_p is the diameter of the plug. The force the plug applies on the stopcock wall can be found by using its relationship with pressure and by determine the contact area.

$$P = \frac{F_p}{A_c}$$

$$F_p = P \cdot A_c$$

$$A_c = \pi \cdot 2r_p \cdot L$$

L is the length of the contact area, and the pressure P is assumed to be the minimum pressure value of 107.5kPa. The frictional torque can then be calculated.

$$T_f = \mu \cdot \left[P(\pi 2 r_p L)\right] \cdot r_p$$

$$T_f = 2\mu \cdot r_p^2 \cdot P \cdot L \cdot \pi$$

$$T_f = 2\pi\ (0.04)\ (0.00396m)^2 (107500Pa)(0.0136m)$$

$$T_f = 0.00576\ Nm$$

The length of the moment arm can then be found by using the following equation:

$$d = \frac{L_h}{2} - d_p \tag{2}$$

According to Ref. [9], the maximum torque that a human finger could produce was approximately 0.015Nm and the maximum force is 2.9N. Realizing that there will be two fingers applying a torque in the same direction and assuming that the frictional torque between the plug and stopcock is 0, we can solve for the minimum length of the handle.

$$T - T_f = F \cdot \left(\frac{L_h}{2} - d_p\right)$$

$$L = 2\left(\frac{2T - T_f}{F} + d_p\right)$$

$$L = 2\left(\frac{0.0242\,\frac{N}{m}}{2.9\ N} + 0.00524m\right)$$

$$L = 27.17mm$$

This result illustrates that the minimum length that the handle can be to turn the plug with all their force is 27.17mm. In order to design this for greater user use, the torque was increased to 0.025Nm to create a scenario in which it is easily turned. Using this torque value, the minimum handle length is 40.99mm.

The maximum radius of the plug can then be found using this current information to determine the radius of the plug that would correspond to a minimum angular velocity of π/s.

$$T = I \cdot \alpha$$

Where I is the moment of the inertia of the plug and α is the angular acceleration. Calculating the moment of inertia using the material properties and assuming that the angular acceleration is 0 to π radians in 1 second the resulting torque is 0.012Nm. From this the radius is 4.15mm. This value is the maximum radius of the plug.

3. Inverted Pendulum

An equation for the simple harmonic motion of the burette can be derived with the assumption of small angles and that the burette stand is clasping around the burette body at point *O* which is a distance *L* away from the end point. The derivation for the harmonic motion of the pendulum is below.

$$I \cdot \ddot{\theta} = \tau \tag{3}$$

I is the rotational moment of inertia of the burette, $\ddot{\theta}$ is the angular acceleration, and τ is the torque. All of these values can be solved for and measured. The angle of the burette can then be found at any point in time with any initial displacement.

$$I = \frac{m \cdot L^2}{12} \tag{4}$$

$$\tau = F_g \cdot d \tag{5}$$

$$\tau = -mg \cdot sin(\theta) \cdot d$$

Plugging in these values we solve for the angular acceleration. In the previous equations *m* is the mass of the burette, *L* is the length of the burette, F_g is the gravitational restoring force of the burette at the center of mass, and *d* is the distance from *O* to the center of mass.

$$\frac{mL^2}{12} \cdot \ddot{\theta} = -mg \cdot \sin(\theta)d$$

$$\ddot{\theta} = -12\frac{g \cdot \sin(\theta) \cdot d}{L^2}$$

$$\ddot{\theta} + 12\frac{g \cdot \theta \cdot d}{L^2} = 0 \tag{6}$$

This is the solution to the simple pendulum of our burette. The position of our burette can be found by assuming that dampening due to air friction is negligible the solution to this equation can be solved. Using the Laplace transform and assuming that the angular acceleration is 0 we get the following equation.

$$\theta(t) = \theta_0 \cdot \cos(\omega t + \phi) \tag{7}$$

$$\omega = \sqrt{\frac{12gd}{L^2}}$$

This equation gives the angular position of the burette at any point in time due to an initial angular displacement. To avoid spilling the burette must have an angular displacement of less than 180°. Due to the sinusoidal nature of the burette and clamp, the only time it will rotate 180° or more is when it has an initial displacement that is equal to or greater than 180° which means that no specific design considerations need to take place as a preventative measure.

If this is an inverted pendulum, then the value d will be smaller than 0 and it will cause the burette system to become very unstable. The equation of motion for the inverted pendulum is the same as the regular pendulum but there are more variables of the system as before [4]. There is an input torque *T*, an effective mass m_f, and a stiffness of the burette housing *k* [5].

$$m_f = \frac{kd}{g} \tag{8}$$

Assuming that the input force is steady state, at time t<0 there is no force acting on it, the center of mass is 40cm away from the rotation point, and there is no initial displacement, the torque resulting from an angular displacement is derived. To torque required to cause the center of mass to accelerate from 0 to 30° is calculated.

$$T = g(m_f - m)\theta \tag{9}$$

$$T = \left(9.81\frac{m}{s^2}\right)\left(\frac{15.646\frac{N}{m}\cdot 0.40m}{9.81\frac{m}{s^2}} - 0.06929\text{kg}\right)\left(\frac{\pi}{6}\right) = 2.9209\ \text{Nm}$$

The maximum forearm and elbow supination and pronation are 16.2 Nm and 13.5 Nm respectively [6]. This result illustrates that it is imperative that the burette is clamped above its center of gravity or else bumping into it accidentally could result it in spilling and accelerating too fast to catch.

4. Energy Analysis

The energy analyses conducted are under the fields of thermodynamics and heat transfer. There are not a profound number of relevant energy analysis that govern the burette, but there are some that dictate tolerances of different mating parts.

1) Hydrostatics

The first energy analysis that was conducted was analyzing the hydrostatic pressure of the burette when it is filled to 50mL. The hydrostatic pressure from the liquid inside of the burette housing will impart a force on two mating components. Those mating components are the plug and the stopcock, and the burette housing and the O-rings. In order for the burette to be leak-proof when it is full the pressure from the interference fits of these two components needs to be greater than this maximum hydrostatic pressure value. Below are the calculations used to find the maximum hydrostatic pressure. The assumptions used in these calculations is that it was steady flow, the liquid was incompressible, the flow was inviscid, and energy loss was negligible.

Using Bernoulli's Equation for conservation of energy:

$$P_1 + \frac{\rho V_1^2}{2} + \rho g z_1 = P_2 + \frac{\rho V_2^2}{2} + \rho g z_2 \tag{10}$$

Where P_1 is the pressure at the top of the burette, P_2 is the pressure of the liquid at the bottom of the burette, ρ is the density of the liquid, V_1 is the initial velocity of the fluid, V_2 is the final velocity of the fluid, z_1 is the height of the fluid at P_1, z_2 is the height of the fluid at P_2, and g is the gravitational constant. Using the assumptions made previously the equation reduces to the following form:

$$P_1 + \rho g z_1 = P_2 + \rho g z_2 \tag{11}$$

Solving for P_2 will determine the maximum hydrostatic pressure for this vessel.

$$P_2 = -\rho g (z_1 - z_2) + P_1 \tag{12}$$

The fluid that was analyzed was liquid water at atmospheric conditions.

$$P_2 = -\left(998\frac{kg}{m^3}\right)\left(9.81\frac{m}{s^2}\right)(0m - 0.585m) + 101.325kPa$$

$$P_2 = 5.727kPa + 101.325kPa$$

$$P_2 = 107.05\ kPa \tag{13}$$

From Eq. (13) it can be determined that the pressure the O-rings exert on the burette housing and the pressure of the plug against the stopcock walls must be greater than 107.05kPa in order to prevent leakage.

The equations used to determine the minimum O-ring diameter are shown below:

$$P_O = \left(\frac{E \cdot F}{\pi L R}\right)^{\frac{1}{2}} \tag{14}$$

This is derived from Hertz contact mechanics between two cylinders. P_O is the pressure caused by the O-ring, E is the modified Youngs Modulus of the O-ring material, L is the contact length, and R is the radius of the O-ring. All of these parameters are known besides the force term which we are going to solve for. We relate material properties to external properties to solve for force as shown below, where σ is the stress and ε is the stress.

$$\sigma = E\epsilon$$

$$\sigma = \frac{F}{A}$$

$$\frac{F}{A} = E\epsilon \tag{15}$$

The contact area A, can be found by determining the contact height between the O-ring and the burette and the length in which it acts over. This height value can be found by applying Pythagorean theorem to the O-ring and burette housing interface and using the parameters of displacement d, and O-ring radius R. The follow expression is then derived using this analysis:

$$R^2 = a^2 + (R - d)^2$$

$$a = \sqrt{2Rd} \tag{16}$$

The displacement value can then be found below:

$$d = (R_O + R) - R_B \tag{17}$$

$$a = \sqrt{2R[(R_O + R) - R_B]}$$

In the above relation R_O is the radius of the O-ring, and R_B is the inner radius of the burette wall. Using the fact that strain is the change in length over the initial length it can be represented in terms of our measured variables above.

$$\epsilon = \frac{d}{(R_O + R)}$$

$$\epsilon = \frac{(R_O+R)-R_B}{(R_O+R)} \tag{18}$$

$$A_c = 2L\sqrt{2R[(R_O + R) - R_B]} \tag{19}$$

Using Eq.18 and Eq.19, the force can be solved for using the following relation:

$$F = 2EL\left(\frac{(R_O+R)-R_B}{R_O+R_B}\right)\sqrt{(2R[(R_O + R) - R_B]} \tag{20}$$

The pressure exerted by the O-ring can now be computed by plugging in the F value into Eq. (15). Plugging in and simplifying produces the following equation where E^* is the modified young's modulus:

$$P_O = \left\{\frac{2^{\frac{3}{2}}\cdot E\cdot E^*\cdot[(R_O+R)-R_B]^{\frac{3}{2}}}{\pi R^{\frac{1}{2}}(R_O+R)}\right\}^{\frac{1}{2}} \tag{21}$$

Plugging in all of the measured values into the equation is shown below.

$$P_O = \left\{ \frac{2^{\frac{3}{2}} \cdot (2.69 \cdot 10^7) \cdot (1.59 \cdot 10^9) \cdot [(0.0048 + 0.00075) - 0.0052]^{\frac{3}{2}}}{\pi\sqrt{0.00075}(0.0048 + 0.00075)} \right\}^{\frac{1}{2}}$$

$$P_O = 4.004\ MPa$$

This is the nominal measurement for a single burette. To calculate the minimum thickness of the O-ring the same equation is used but the variable R is left to be unknown, and it is solved for by using a simultaneous solutions method. Using this method, the minimum thickness the O-ring needs to be in order to prevent leakage is 0.8mm. Conversely, this means that the inner diameter of the burette wall needs to have an inner radius of at least 5.2mm.

This same process can be used to determine the minimum diameter of the plug in order to resist the force of gravity to prevent it from falling out of the plug hole. Plugging in all the values for the handle and the plug we get that the minimum radius of the handle is 3.04mm.

Additionally, the plug that is inserted into the stopcock body needs to be leakproof. The hoop stress exerted on the stopcock body can be equated to Hooke's Law resulting in:

$$\sigma_H = \frac{Pr}{t} \tag{22}$$

$$\epsilon E = \frac{Pr}{t} \tag{23}$$

This can be solved for *P* and used to define a minimum radius value for the plug. First the strain needs to be defined using the following equation:

$$\epsilon = \frac{r - r_s}{r} \tag{24}$$

Where *r* is the radius of the plug, r_s is the radius of the stopcock wall, *t* is the thickness of the stopcock wall, and *E* is the young's modulus of the plug. This results in the following equation which can be solved for r since all the other properties are known.

$$P = \frac{\left(\frac{r - r_s}{r}\right) Et}{r} \tag{25}$$

$$P = \frac{\left(\frac{r - 0.00387m}{r}\right) (0.392 \cdot 10^9)\ (0.00165m)}{r}$$

Using a simultaneous solution method, r is found to be 3.9mm. This is the minimum radius of the plug in order to prevent leakage. The minimum inner radius of the stopcock body is 3.87mm.

5. Fluids Analysis

1) Bernoulli's Drain

The drain time for the burette can be calculated using Bernoulli's equation. The equation can be simplified to the following form:

$$\frac{\rho V_1^2}{2} + \rho g h(t) = \frac{\rho V_2^2}{2}$$

$$g h(t) = \frac{V_2^2 - V_1^2}{2}$$

Knowing that the volumetric flow rates need to be equal between the different sections, we can solve for the outlet velocity in terms of the cross-sectional areas and the inlet velocity.

$$V_2 = \frac{A_1}{A_2} V_1 \tag{26}$$

$$V_1 = -\frac{dh}{dt}$$

The rate of change of the liquid column height can then be found using the following equation.

$$\frac{dh}{dt} = \sqrt{\frac{2gh(t)}{\left(\frac{A_1}{A_2}\right)^2 - 1}} \tag{27}$$

The differential equation can be solved using the separation of variables technique and this results in the following.

$$-\int \sqrt{\frac{2g}{\left(\left(\frac{A_1}{A_2}\right)^2 - 1\right)}}\, dt = \int \frac{1}{\sqrt{h(t)}}\, dh \tag{28}$$

Solving this for t will result in the time it takes to drain.

$$t = \frac{2h_o^{0.5}}{\sqrt{\frac{2g}{\left(\left(\frac{d_1}{d_2}\right)^4 - 1\right)}}} \tag{29}$$

To solve for the drain time the initial condition of height needs to be measured. Plugging in all of the measured variables results in the following time.

$$t = \frac{2\sqrt{0.585m}}{\sqrt{\frac{2\left(9.81\frac{m}{s^2}\right)}{\left(\left(\frac{0.01051}{0.00104}\right)^4 - 1\right)}}}$$

$$t = 35.267s$$

For a burette full of liquid water, it will take it approximately 35.267 seconds. This result was also compared against values resulting from real world analysis on the drain time. For 10 different iterations the mean drain time was 39.43 seconds. This discrepancy between the theoretical and tested values can be explained by factors not taken into consideration such as the friction of the acrylic wall and the force due to surface tension.

The maximum nozzle diameter can be solved for by choosing a time of 25 seconds to be the minimum allowed time for the draining of the burette the nozzle diameter needs to be less than 1.235mm in diameter.

2) Surface Tension Forces

The minimum nozzle diameter can then be solved for using a force balance between the surface tension and the force of gravity on the body of water. First the equation for surface tension will be stated and then the derivation for the max weight of the water.

$$F_s = 2\pi \cdot s \cdot cos(\theta) \tag{30}$$

$$F_g = \pi r_n^2 h \rho g \tag{31}$$

Where h is the height of the water column, s is the surface tension of water, F_s is the upward force due to surface tension, F_g is the force due to gravity, θ is the contact angle between the liquid and the burette wall, and r_n is the nozzle radius. Now knowing that the force due to tension needs to be less than the force due to gravity we set the two terms equal and solve for the nozzle radius.

$$\pi r_n^2 h \rho g = 2\pi \cdot s \cdot cos(\theta)$$

$$r_n = \sqrt{\frac{2 \cdot s \cdot \cos(\theta)}{\rho g h}}$$

For the minimum water height of 0.1m the nozzle radius can be found.

$$r_n = \sqrt{\frac{2 \cdot \left(0.07275 \frac{J}{m^2}\right) \cdot \cos(45°)}{\left(998 \frac{kg}{m^3}\right)\left(9.81 \frac{m}{s^2}\right)(0.1m)}}$$

$$r_n = 0.0001048m$$

This radius of the nozzle needs to be greater than this value in order for water to flow out of the nozzle. The minimum nozzle diameter must be greater than 0.211mm.

6. Mechanical Design Analysis

1) Failure Moment of Burette.

The amount of force required to break and destroy the burette is an important quantity. Tapping the burette nozzle on the side of a beaker causes an impulse force that has the potential to rupture the burette if it is large enough. The burette will be treated as a cantilever beam that has the same moment of inertia as a hollow rod about the y-axis. The bending stress for this analysis is below. M is the moment applied to the beam, S is the flexural modulus of the burette, and σ_{max} is the breaking stress.

$$\sigma_{max} = \frac{M}{S} \tag{32}$$

$$\sigma_{max} \cdot S = M$$

$$F = \frac{\sigma_{max} \cdot S}{L}$$

$$S = \frac{\pi(d_o^4 - d_i^4)}{32 \cdot d_o}$$

$$F = \frac{(75 \cdot 10^6 Pa)(2.36 \cdot 10^{-7}\ kg \cdot m^2)}{(0.67978m)} = 26.037\ N.$$

The maximum force that can be applied that would cause rupture is 26.037N. This is equivalent to 2.654 kg hanging down on the end. This differs from the tested maximum force. The burette was tested, and it failed after 5.62kg was hung from the end. This is equivalent to 55.132N being applied to the end of the burette. The tested force at failure is 2.117 times larger than the theoretical force at failure. This is a large amount of force and is greater than other forces for different burette materials. For example, Pyrex has a fracture stress of about 29 MPa which results in the force at failure to be 10.1 N [3]. This is less than half of the failure force of the acrylic burette. The maximum weight that could fall on this burette is 2.2lbs which is barely higher than the average weight of a human hand (1.03lbs) [2].

2) Fatigue Life of Acrylic Burette

The number of cycles to failure for this burette can be calculated for varying impulse stresses applied to the acrylic (PMMA) body.

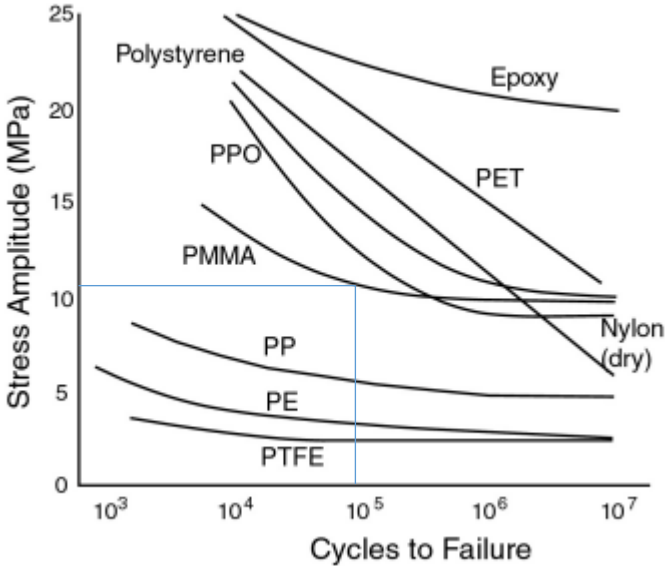

Figure 14: S-N Curve for Different Materials [1]

Using three-fourths of the experimental force at fracture, a measured contact area, and the curve above the number of times it would take to fail the part can be calculated.

$$\frac{\sigma_m}{\sigma_{ULT}} + \frac{\sigma_a}{\sigma_N} = 1 \tag{33}$$

The cyclic stress needs to be calculated to determine the cycles to failure. The mean stress is 0 so the cyclic stress is the same as the stress amplitude. Calculating the stress amplitude results in the following.

$$\sigma_a = \frac{F_a}{A_c}$$

$$\sigma_a = \frac{40\ N}{3.941 \cdot 10^{-6}\ m^2} = 10.1\ MPa$$

Utilizing the S-N curve the number of cycles to failure for this specific stress amplitude is 10^5. The burette needs to be hit 100,000 times with a force of 40N before it would fail. This is an extremely long time and is not realistic in terms of its daily use.

3) Buckling Critical Stress

The critical stress that causes buckling of the acrylic burette body if it was dropped from a certain height is determined below. P is the load imposed on the burette and A is the cross-sectional area.

$$\sigma_{cr} = \frac{P}{A} \tag{34}$$

$$P = \frac{\pi^2 EI}{L^2} \tag{35}$$

$$A = \pi(r_o^2 - r_i^2)$$

$$A = \pi(14.99^2 mm - 10.97^2 mm) = 81.96\ mm^2$$

$$I = \frac{\pi}{2}(r_o^2 + r_i^2) \tag{36}$$

$$I = \frac{\pi}{2}(0.00747^4 + 0.005485^4) = 9916.14 \cdot 10^{-12} m^4$$

$$\sigma_{cr} = 20.278\ MPa$$

The burette housing would buckle if it experienced more than 20.278 MPa of stress on it. The same analysis can apply for the nozzle, and it will be treated as a hollow cylinder to find the moment of inertia.

$$I = \frac{\pi}{2}(0.00128^4 + 0.000563^4) = 6.8712 \cdot 10^{-12} m^4$$

$$A = \pi(1.28^2 mm - 0.563^2 mm) = 1.32\ mm^2$$

$$\sigma_{cr} = 0.118\ MPa$$

7. Most Prevalent Failure Modes

Previous failure analyses determined various failure modes for the burette and now the most probably one will be determined. The failure modes consist of impulse force reaction, fatigue life, and buckling. The mode that is most likely to occur is the buckling mode of failure for the nozzle specifically. The nozzle had a critical stress of 0.118 MPa and this is the smallest stress value out of all the failure analyses. Given the contact areas and all relevant measurements this is the most achievable stress on a day-to-day basis for the burette. If the burette falls from 2.5 meters than it will buckle and it will no longer be usable. This is a much more likely scenario that someone hitting the burette 100,000 times on the side of the beaker to cause failure. It is also much more likely that imposing 55N of force on the edge of the burette tip by hitting it swiftly. This is extremely difficult to do even if it was intended.

Therefore, the most probable cause for failure in the burette assembly is for it to be dropped and then buckle due to the impact force from colliding with the ground. Additionally, the nozzle is made from PP which is injection molded. This means that it is produced from the manufacturing method that reduces its strength the most out of the other manufacturing processes used and it increases the likelihood of this failure mode to occur.

8. DML Analysis

1) Manufacturing Analysis

The manufacturing methods used to produce all of the separate parts in this assembly mainly consisted of injection molding. The stopcock, handle and the nozzle all use injection molding. The only parts that differ in the manufacturing process are the O-rings, plug and the Burette housing.

Injection molding is performed by injecting melted plastic (PP or PE in our case) into a mold of a desired geometry. When the plastic cools and hardens it takes the form of the mold and it is taken out to be inspected. There are a lot of benefits to using this manufacturing process because it is easier to make parts in bulk since you can make lots of the same molds, it is cheap since it mainly just deals with plastics and they are much easier to maintain, buy, and manufacture, and it isn't a hazardous process. Some of the drawbacks for this method include the fact that when plastic cools down it expands so it produces a lot of uncertainty with this process. There is approximately 0.0127mm of tolerance that need to be taken into consideration when using injection molding [7]. Another limitation is the production of these molds for the plastics. If the desired part has extremely complex geometry and it is extremely large the mold will take a lot of resources to build accurately and the cooling down for the plastic mold will increase exponentially.

For parts like the O-rings which are made of Styrene, the manufacturing processes that are used mainly consist of compression molding, injection molding, and transfer molding. The process that produced these O-rings was compression molding since it is more common for natural rubbers and elastomers. The compression mold process essentially places the material in a mold cavity and then it is closed with increasing heat and pressure. This causes the material to form the shape of the mold and since the melting point is a function of both pressure and time there is a lot more control in this process than injection molding. Additionally, for simple geometries such as the torus O-ring shape, compression molds are better suited to manufacturing these than injection molding because it is a lot simpler. Some of the disadvantages of using this method is that it is a slower process because it takes longer for the part to cure after the mold, and it shouldn't be used for complex parts because it will take much longer to mold the part to a specific geometry compared to injection molding [18]. The tolerances that accompany this manufacturing process are ± 0.102mm [21].

The acrylic burette housing body uses a different manufacturing technique than the other parts. While acrylic can be manufactured using injection molding it is smarter to use thermoforming to shape the acrylic instead. Injection molding weakens the acrylic and makes it more brittle than thermoformed acrylic. The thermoformed acrylic body has a smaller surface roughness and tolerance than injection molding. This process is also well suited for larger products that need to be manufactured such as the acrylic burette body. Some of the key disadvantages of thermoforming is that it is much more expensive than other methods and it isn't as conservative in terms of material usage [19]. The process of thermoforming produces a lot of variation in tolerances due to the type of thermoforming being done and the part geometry. The acrylic feature is thermoformed in a vacuum and all of the dimensions are formed features which means that there is a ±0.3mm tolerance [22].

The plug is made of PTFE and this material cannot be injection molded. PTFE will not flow when it is raised above its melting point due to the extremely high viscous forces present in the material. The alternative to this is to compress the PTFE powder into smaller molds. These pre-molds are then placed in the assembly mold where it is heated and pressurized to the point where it sinters and adheres together. This is a much more costly process since it

has more steps than other processes and each of these steps take longer due to the fact that it is being compressed and pressurized instead of melted. It is able to produce various geometric shapes and can do so in large quantities. Sometimes the parts need to go through another adhering process where they weld/fuse these different PTFE assembly molds together to manufacture the last version [20]. Due to the various processes that comprise the manufacturing of PTFE there is a tolerance stack-up that ultimately results in this process having the highest tolerance since it has the tolerances due to post manufacturing methods and it uses compression molding which produces the most tolerance out of the other manufacturing methods.

2) Manufacturing Failure Analysis

When the burette is in use and filled with liquids the burette body will experience a pressure at its new center of mass. The density of the liquid will cause the variance of this pressure and it is wise to calculate what density would cause plastic strain in the burette body. This is an important design aspect since if the burette body deforms plastically then the graduation marks will be incorrect since there is a reduction in the cross-sectional area at that deformation point. In order to avoid that the burette body needs to have a certain yield strength, a maximum density of liquid being used to titrate, or a combination of both. Using the weight of gravity as the force that's acting on the burette body and solving for the density the following is derived. The yield strength of acrylic is used for the analysis which is 48.9MPa [23]. Additionally, the center of mass is assumed to be inside of the burette wall assembly so the cross-sectional area can be calculated.

$$F = ma$$

$$F = \rho V g$$

$$\sigma_{yield} = \frac{F}{A_c}$$

$$\sigma_{yield} \cdot A_c = F$$

$$\sigma_{yield} \cdot \left(\pi(r_o^2 - r_i^2)\right) = \rho V g$$

$$\rho = \frac{\sigma_{yield} \cdot \left(\pi(r_o^2 - r_i^2)\right)}{Vg} \tag{37}$$

The density that would cause the burette to yield can then be found by plugging in all of the know parameters into Eq. 37.

$$\rho = \frac{(48.9 \cdot 10^6\ Pa) \cdot \left(\pi(0.00746^2\ m^2 - 0.00546^2 m^2)\right)}{(5 \cdot 10^{-5} m^3)\left(9.81 \frac{m}{s^2}\right)} = 8093.05 \frac{g}{cm^3}$$

The maximum liquid density for a 50mL titration is 8093.05 g/cm^3. Considering that the densest liquid is mercury at about 13.6 g/cm^3, yielding is almost impossible to occur regardless of the type of liquid you wish to use as a titrant [24].

Another analysis that can be performed is to determine the radius of the nozzle press fit to the stopcock inner diameter. If the force of friction is less than the hydrostatic force the filled burette imposes on it the nozzle will fall off. There needs to be some interference regardless of if it is filled because it would stay fastened if wasn't a press or a snap fit. Using Eq.20 and the hydrostatic pressure value from Eq.13 the minimum diameter of the nozzle can be determined. The coefficient of static friction for PP is 0.46.

$$F_f > F_{hydro}$$

$$F_f = \mu_s \cdot 2EL\left(\frac{(R_O + R) - R_B}{R_O + R_B}\right)\sqrt{(2R[(R_O + R) - R_B]} \tag{38}$$

Using a simultaneous solutions method, the minimum radius can be found. The solution was found vie graphing and the intersection was found to be 0.002508 which corresponds to 2.508mm. The maximum radius is found using

tolerance loops. The measured radius of the nozzle was found to be 3.805mm which is 65% larger than the minimum size and it is determined that the nozzle won't become dismembered from the stopcock.

3) Assembly Analysis

The ease of assembly also needs to be designed for because it has the potential to be catastrophic in terms of production quantities, production qualities, and wasted materials. The most ideal form of fastening and assembling two mating parts is by using an interference/press fit. This is because there are no parts that need to be screwed, welded, or adhered any other way which would dramatically increase assembly time per part. This burette assembly has 10 unique interference fits which complete the entire assembly. This is the most optimal fastening method and increases the production flow substantially.

Another factor is the weight and fragility of the assembly parts. If the part weighs a considerable amount, then it leads to longer assembly time and faster assembly fatigue. The burette is comprised mainly of plastic which has an average density that is lower than other materials such as glass and metals. This means that the burette is lightweight and doesn't require much effort to assembly. The fragility of parts is also an important aspect of assembly due to the fact that extra time will be required to ensure the proper assembly of the part so failure doesn't occur. Common accidents such as dropping parts or hitting parts together could cause failure in the part which means that it needs to be scrapped since the assembly wont function correct if one part has failed (for this burette except for the 3 large O-rings). The large breaking stress and yield stress of the plastics that are used indicate that the burette isn't fragile in any capacity and the parts can be handled without caution.

IV. Dimensional Analysis

The determination of the tolerances for certain functional interfaces and surfaces was found using tolerance loops. Known nominal measurements were taken by using the caliper or by using equal distribution between tolerance limits. The tolerances on certain vectors/parts were found by determining the manufacturing method and the corresponding accuracy. Many of these parts are modeled using injection molding which has a 0.0127mm tolerance range [7]. Other tolerances were found via engineering analyses that were conducted on the assembly interfaces and what values are within the laws of physics for the burettes original design intent.

A. Tolerance Loop 1- Large O-ring, Stopcock, and Burette Wall

The interference fit between the large O-rings in the stopcock grooves and the inner burette housing walls is a functional surface. If this interference fit is too large, then it won't be leak proof and if it is too big then it will be too difficult to disassemble and reassemble. These analyses will calculate the maximum interference size, and the tolerance range for the entire radius.

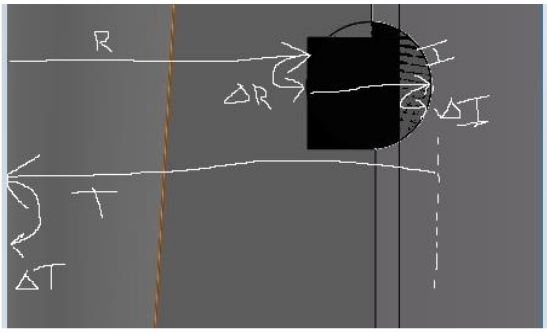

Tolerance Loop 1

Vector Name	Nominal Dimension (mm)	Tolerances		Reference
R	4.150	+Δx1	0.0127	Injection Mold / Caliper
		-Δx1	0.0127	Injection Mold / Caliper
I	1.805	+Δx2	ΔI	Caliper Measured
		-Δx2	0.5025	Caliper Measured/ hyrdostatic analysis
T	5.590	+Δx3	ΔT	Caliper Measured
		-Δx3	ΔT	Caliper Measured
		+Δx4		
		-Δx4		
		+Δx5		
		-Δx5		
		+Δx6		
		-Δx6		
		+Δx7		
		-Δx7		
		+Δx8		
		-Δx8		
		+Δx9		
		-Δx9		
		+Δx10		
		-Δx10		
		+Δx11		
		-Δx11		
		+Δx12		
		-Δx12		

Figure 15: Tolerance Loop 1

$$(\bar{R} \pm \Delta\bar{R}) + (\bar{I} \pm \Delta\bar{I}) + (\bar{T} \pm \Delta\bar{T}) = 0$$

$$T_{max} = (R + \Delta R) + (I + \Delta I) \tag{39}$$

$$T_{min} = (R - \Delta R) + (I - \Delta I) \tag{40}$$

Using these equations, the tolerances for the O-ring and the interference can be calculated.

$$T_{min} = (4.150 - 0.0127) + (1.805 - 0.5025) = 5.439mm$$

$$T_{max} = T + \Delta T = 5.741mm$$

$$I_{max} = T_{max} - (R + \Delta R) = 1.850mm$$

The resulting maximum interference is 0.50mm and the tolerances of the interference radii are ±0.151mm. These tolerances are put into place to retain a liquid tight seal for the burette and to increase its ease of overall use.

New manufacturing methods or materials could improve these tolerances and create more reliable designs. The injection molding process allows for lots of uncertainty to arise in the assemblies and should be improved to save on material costs.

B. Tolerance Loop 2-Small O-ring and Plug

The interface of the plug body, O-ring, and the O-ring groove is a functional surface. This is what determines whether or not the plug will dislodge out of the stopcock easily and is used to ensure there is enough room for the O-ring groove to be easily accessible and functional. The values that will be calculated are the tolerances of the gap between the O-ring groove and the stopcock body.

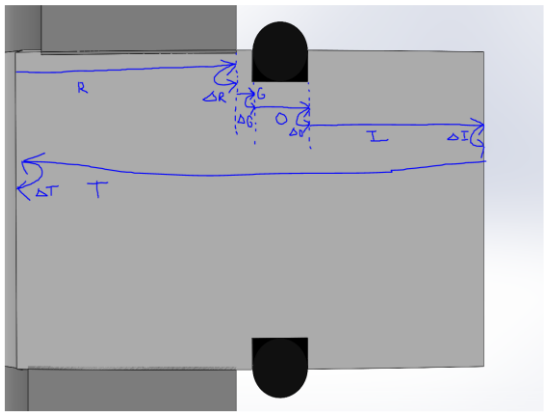

Tolerance Loop 2

Vector Name	Nominal Dimension (mm)	Tolerances		Reference
R	5.810	+Δx1	0.0127	Injection Molding/ Caliper Measured
		-Δx1	0.0127	Injection Molding/ Caliper Measured
G	-	+Δx2	ΔG	
		-Δx2	ΔG	
O	1.600	+Δx3	0.0127	Injection Molding/ Caliper Measured
		-Δx3	0.0127	Injection Molding/ Caliper Measured
I	4.680	+Δx4	0.0127	Injection Molding/ Caliper Measured
		-Δx4	0.0127	Injection Molding/ Caliper Measured
T	12.250	+Δx5	0.0127	Injection Molding/ Caliper Measured
		-Δx5	0.0127	Injection Molding/ Caliper Measured
		+Δx6		
		-Δx6		
		+Δx7		
		-Δx7		
		+Δx8		
		-Δx8		
		+Δx9		
		-Δx9		
		+Δx10		
		-Δx10		
		+Δx11		
		-Δx11		
		+Δx12		
		-Δx12		

Figure 16: Tolerance Loop 2

$$(\bar{R} \pm \Delta\bar{R}) + (\bar{G} \pm \Delta\bar{G}) + (\bar{O} \pm \Delta\bar{O}) + (\bar{I} \pm \Delta\bar{I}) + (\bar{T} \pm \Delta\bar{T}) = 0$$

$$G_{max} = (T + \Delta T) - [(R - \Delta R) + (O + \Delta O) + (I - \Delta I)] \quad (41)$$

$$G_{min} = (T - \Delta T) - [(R + \Delta R) + (O - \Delta O) + (I + \Delta I)] \quad (42)$$

Using Equations 25 and 26 the maximum and minimum gap value can be found.

$$G_{max} = (12.25 + 0.0127) - [(5.81 - 0.0127) + (1.60 + 0.0127) + (4.68 - 0.0127)] = 0.1854mm$$

$$G_{max} = (12.25 - 0.0127) - [(5.81 + 0.0127) + (1.60 - 0.0127) + (4.68 + 0.0127)] = 0.1346mm$$

The resulting tolerances range by only 0.05mm. This is an extremely tight tolerance and in order to increase this range the manufacturing methods need to be increased. Injection molding results in high tolerance and will restrict this specific tolerance to the point where it will be extremely difficult to assemble this product.

C. Tolerance Loop 3- Plug and Stopcock

The interference fit interface between the plug and the stopcock wall is a functional surface. If the plug is too small, then it won't produce enough pressure to be watertight and if it is too large then it will be difficult to turn. The tolerance analysis will be used to solve for the range of values for the stopcock inner diameter.

Tolerance Loop 3

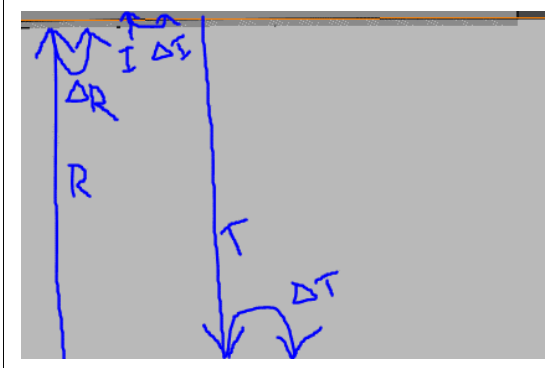

Vector Name	Nominal Dimension (mm)	Tolerances		Reference
R	7.310	+Δx1	ΔR	Caliper Measure/ Injection Mold
		-Δx1	ΔR	
I	0.620	+Δx2	0.0127	Dynamics Analysis
		-Δx2	0.0127	Hydrostatics Analysis
T	7.930	+Δx3	0.3700	Caliper Measure/ Injection Mold
		-Δx3	0.1900	Caliper Measure/ Injection Mold
		+Δx4		
		-Δx4		
		+Δx5		
		-Δx5		
		+Δx6		
		-Δx6		
		+Δx7		
		-Δx7		
		+Δx8		
		-Δx8		
		+Δx9		
		-Δx9		
		+Δx10		
		-Δx10		
		+Δx11		
		-Δx11		
		+Δx12		
		-Δx12		

Figure 17: Tolerance Loop 3

$$(\bar{R} \pm \Delta\bar{R}) + (\bar{I} \pm \Delta\bar{I}) + (\bar{T} \pm \Delta\bar{T}) = 0$$

$$R_{max} = -(I - \Delta I) + (T + \Delta T) \tag{43}$$

$$R_{min} = -(I + \Delta I) + (T - \Delta T) \tag{44}$$

Using these equations, the range of radius values of the stopcock inner diameter can be found

$$R_{max} = -(0.620 - 0.0127) + (7.930 + 0.370) = 7.667mm$$

$$R_{min} = -(.620 + 0.0127) + (7.930 - 0.190) = 7.107mm$$

The stopcock inner diameter needs to range from 7.107mm to 7.667mm in order to maintain the liquid tight-seal and to enable easy rotation of the plug inside the stopcock. Due to the extensive range of this diameter the manufacturing processes will make this easy to maintain and they don't need to be altered.

D. Tolerance Loop 4- Handle and Plug

The handle and plug interference fit is a functional surface. The handle diameter needs to be greater than the plug inner diameter in order to prevent the handle from falling out of the plug due to the force of gravity. The interference will be measured in the following tolerance loop.

Tolerance Loop 4

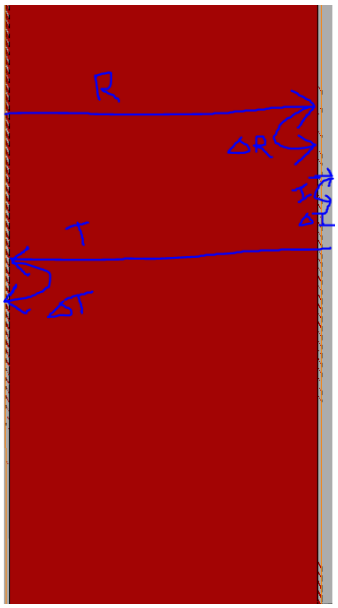

Vector Name	Nominal Dimension (mm)	Tolerances		Reference
R	3.025	+Δx1	0.0127	Caliper Measured/ Injection Molding
		-Δx1	0.0127	Caliper Measured/ Injection Molding
I	0.210	+Δx2	ΔI	
		-Δx2	ΔI	
T	3.235	+Δx3	ΔT	
		-Δx3	0.1950	Force Analysis/ Caliper Measured
		+Δx4		
		-Δx4		
		+Δx5		
		-Δx5		
		+Δx6		
		-Δx6		
		+Δx7		
		-Δx7		
		+Δx8		
		-Δx8		
		+Δx9		
		-Δx9		
		+Δx10		
		-Δx10		
		+Δx11		
		-Δx11		
		+Δx12		
		-Δx12		

Figure 18: Tolerance Loop 4

$$(\bar{R} \pm \Delta\bar{R}) + (\bar{I} \pm \Delta\bar{I}) + (\bar{T} \pm \Delta\bar{T}) = 0$$

$$I_{max} = -(R - \Delta R) + (T + \Delta T) \tag{45}$$

$$I_{min} = -(R + \Delta R) + (T - \Delta T) \tag{46}$$

The tolerance range for the interference fit and the upper tolerance limit for the handle can be found using equations 29 and 30.

$$I_{max} = -(3.025 - 0.0127) + (3.235 + \Delta T)$$

$$\Delta T = -(3.025 - 0.0127) + (3.235) - (0.210 + 0.0023)$$

$$I_{min} = -(3.025 + 0.0127) + (3.235 - 0.1950) = 0.0023mm$$

Assuming an equal distribution of tolerances about the interference vector I_{max} is 0.2123mm. The upper tolerance limit for the handle was found to be 3.2454mm. There is 0.205mm of range in which this handle can be manufactured in order to prevent it from falling out of the plug hole and to satisfy all of the other dimensional requirements and tolerances.

E. Tolerance Loop 5- Plug and Stopcock Gap

The interface between the plug larger outer diameter and the stopcock is a functional surface. There needs to be a gap in order for the burette to be assembled properly without the plug not being able to enter fully. The gap between these two quantities will be solved for in the following tolerance loop. The minimum gap that can occur is a gap of 0mm.

Tolerance Loop 5

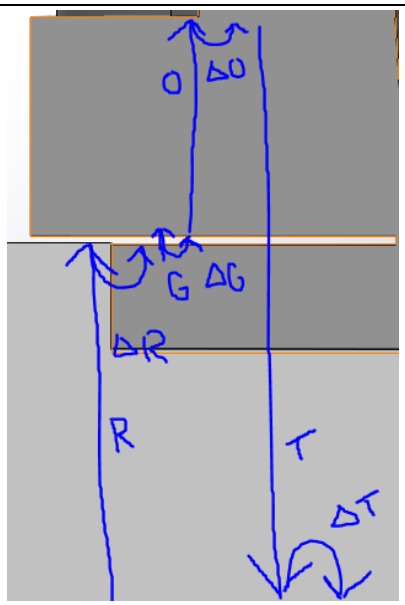

Vector Name	Nominal Dimension (mm)	Tolerances		Reference
R	6.075	+Δx1	0.0127	Caliper Measured/ Injection Molding
		-Δx1	0.0127	Caliper Measured/ Injection Molding
G	0.420	+Δx2	ΔG	
		-Δx2	0.4200	
O	3.760	+Δx3	0.0127	Caliper Measured/ Injection Molding
		-Δx3	0.0127	Caliper Measured/ Injection Molding
T	10.225	+Δx4	ΔT	Caliper Measured/ Injection Molding
		-Δx4	ΔT	
		+Δx5		
		-Δx5		
		+Δx6		
		-Δx6		
		+Δx7		
		-Δx7		
		+Δx8		
		-Δx8		
		+Δx9		
		-Δx9		
		+Δx10		
		-Δx10		
		+Δx11		
		-Δx11		
		+Δx12		
		-Δx12		

Figure 19: Tolerance Loop 5

$$(\bar{R} \pm \Delta\bar{R}) + (\bar{O} \pm \Delta\bar{O}) + (\bar{G} \pm \Delta\bar{G}) + (\bar{T} \pm \Delta\bar{T}) = 0$$

$$\Delta T = T - (R + \Delta R) - (G - \Delta G) - (O + \Delta O) \tag{47}$$

$$G_{max} = -[(R - \Delta R) + (O - \Delta O)] + (T + \Delta T) \tag{48}$$

The tolerances can be found by using Equations 31. And 32.

$$\Delta T = -(6.075 + 0.0127) - (0.420 - 0.0420) - (3.76 + 0.0127) + 10.225 = 0.3646mm$$

$$G_{max} = -[(6.075 - 0.0127) + (3.76 - 0.0127)] + (10.225 + 0.3646) = 0.78mm$$

The gap between the stopcock body and the plug outer radius ranges from 0mm to 0.78mm. This is the amount of space required for the burette to be fully assembled without any issues. The manufacturing methods do not need to be altered because they provide enough precision to achieve this gap tolerance.

F. Tolerance Loop 6- Nozzle

The nozzle hole is a functional surface. The inner diameter of the hole needs to be a certain diameter to allow for water to flow at a certain volumetric weight and to overcome the surface tension. The thickness range of the nozzle diameter is calculated below using the following tolerance loop.

Tolerance Loop 6

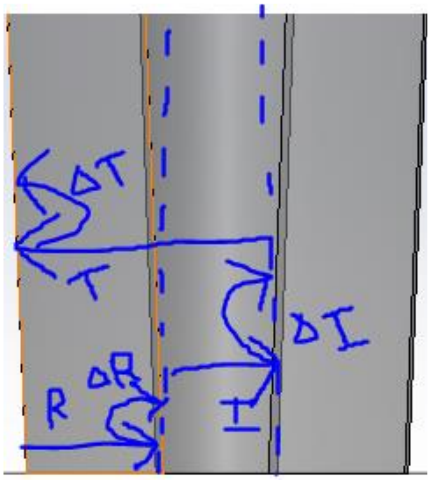

Vector Name	Nominal Dimension (mm)	Tolerances		Reference
R	1.060	+Δx1	ΔR	
		-Δx1	ΔR	
I	0.723	+Δx2	0.5120	Volumetric Flow Rate Analysis
		-Δx2	0.5120	Surface Tension Analysis
T	2.220	+Δx3	0.0127	Caliper Measured/ Injection Mold
		-Δx3	0.0127	Caliper Measured/ Injection Mold
		+Δx4		
		-Δx4		
		+Δx5		
		-Δx5		
		+Δx6		
		-Δx6		
		+Δx7		
		-Δx7		
		+Δx8		
		-Δx8		
		+Δx9		
		-Δx9		
		+Δx10		
		-Δx10		
		+Δx11		
		-Δx11		
		+Δx12		
		-Δx12		

Figure 20: Tolerance Loop 6

$$(\bar{R} \pm \Delta\bar{R}) + (\bar{I} \pm \Delta\bar{I}) + (\bar{T} \pm \Delta\bar{T}) = 0$$

$$R_{max} = (T + \Delta T) - (I - \Delta I) \tag{49}$$

$$R_{min} = (T - \Delta T) - (I + \Delta I) \tag{50}$$

The range for the thickness of the nozzle can then be solved for using Eq. 33 and Eq. 34.

$$R_{max} = (2.220mm + 0.0127\text{mm}) - (0.723mm - 0.5120\text{mm}) = 2.022mm$$

$$R_{min} = (2.220mm - 0.0127\text{mm}) - (0.723mm + 0.5120\text{mm}) = 0.9723mm$$

The thickness of the nozzle can range over 1mm and isn't sensitive to the other dimensional constraints. The volumetric flow rate time can be achieved using the current injection molding manufacturing method and doesn't need any alterations.

G. Tolerance Loop 7- Burette Housing and Handle

The handle and burette housing gap are a functional surface. There needs to be a gap between these two parts or else the burette won't function properly because the handle would be hitting the burette housing with every 180-degree rotation. The gap range between these two parts is found below using a tolerance loop analysis.

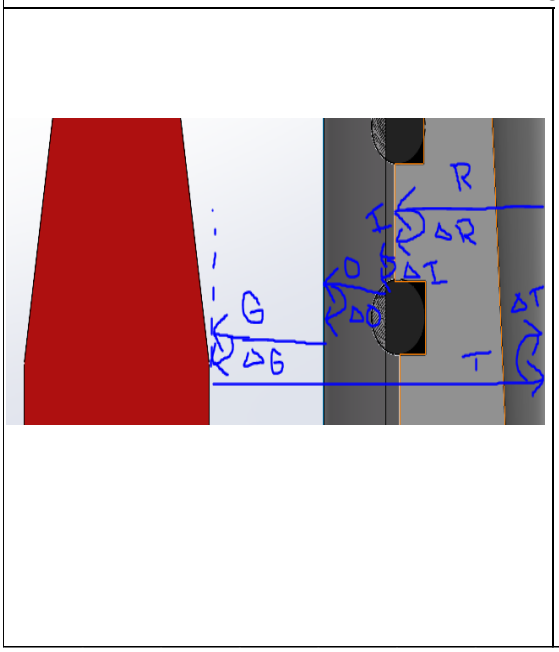

Tolerance Loop 7

Vector Name	Nominal Dimension (mm)	Tolerances		Reference
R	5.105	+Δx1	0.0127	Caliper Measured/ Injection Mold
		-Δx1	0.0127	Caliper Measured/ Injection Mold
I	0.330	+Δx2	0.0127	Caliper Measured/ Injection Mold
		-Δx2	0.3300	
O	1.870	+Δx3	0.0127	Caliper Measured/ Injection Mold
		-Δx3	0.0127	Caliper Measured/ Injection Mold
G	4.030	+Δx4	ΔG	Caliper Measured
		-Δx4	4.0300	
T	11.515	+Δx5	ΔT	Caliper Measured
		-Δx5	ΔT	
		+Δx6		
		-Δx6		
		+Δx7		
		-Δx7		
		+Δx8		
		-Δx8		
		+Δx9		
		-Δx9		
		+Δx10		
		-Δx10		
		+Δx11		
		-Δx11		
		+Δx12		
		-Δx12		

Figure 21: Tolerance Loop 7

$$(\bar{R} \pm \Delta\bar{R}) + (\bar{I} \pm \Delta\bar{I}) + (\bar{O} \pm \Delta\bar{O}) + (\bar{G} \pm \Delta\bar{G}) + (\bar{T} \pm \Delta\bar{T}) = 0$$

$$G_{max} = (T + \Delta T) - [(R - \Delta R) + (O - \Delta O) + (I - \Delta I)] \quad (51)$$

$$\Delta T = T - [(R + \Delta R) + (O + \Delta O) + (I + \Delta I) + (G - \Delta G)] \quad (52)$$

Using Eq. 35 and Eq.36 the tolerance range for the T vector can be found and the upper limit for the gap can be found.

$$\Delta T = 11.515 - [(5.105 + 0.0127) + (1.87 + 0.0127) + (0.33 + 0.0127) + (4.030 - 4.030)] = 4.172mm$$

$$G_{max} = (11.515 + 4.172) - [(5.105 - 0.0127) + (1.87 - 0.0127) + (0.330 - 0.330)] = 8.7274mm$$

The minimum gap that is allowed for this burette to function is 0mm since nothing would be impeded. This results in the overall length to vary by 4.172mm and this results in the maximum gap between the handle and the burette housing to be 8.7274mm. This large gap range illustrates that this isn't a tight dimension that needs to be modified or changed due to the current manufacturing methods. There is ample room for increases in tolerance before this functional surface is in jeopardy.

H. Tolerance Loop 8- Nozzle and Stopcock

In order for the nozzle to remain on the stopcock and not fall off when it is filled with liquid there needs to be an interference fit. This is a functional surface and the max and min values for this interference needs to be found using tolerance loops. The nozzle outer diameter needs to be bigger and elastically deform inside the smaller stopcock inner diameter.

Tolerance Loop 8

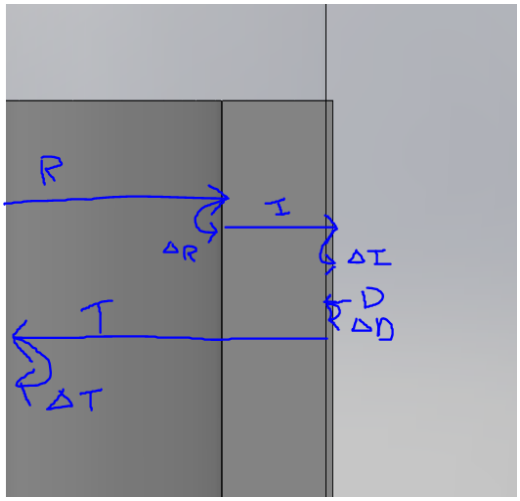

Vector Name	Nominal Dimension (mm)	Tolerances		Reference
R	2.010	+Δx1	0.0127	Caliper Measured/ Injection Mold
		-Δx1	0.6860	Engineering Analysis
I	0.920	+Δx2	0.0127	Caliper Measured/ Injection Mold
		-Δx2	0.0127	Caliper Measured/ Injection Mold
D	0.100	+Δx3	ΔD	Caliper Measured/ Injection Mold
		-Δx3	ΔD	Caliper Measured/ Injection Mold
T	3.110	+Δx4	0.0127	Caliper Measured/ Injection Mold
		-Δx4	0.0127	Caliper Measured/ Injection Mold
		+Δx5		
		-Δx5		
		+Δx6		
		-Δx6		
		+Δx7		
		-Δx7		
		+Δx8		
		-Δx8		
		+Δx9		
		-Δx9		
		+Δx10		
		-Δx10		
		+Δx11		
		-Δx11		
		+Δx12		
		-Δx12		

Figure 22: Tolerance Loop 8

$$(\bar{R} \pm \Delta\bar{R}) + (\bar{O} \pm \Delta\bar{O}) + (\bar{G} \pm \Delta\bar{G}) + (\bar{T} \pm \Delta\bar{T}) = 0$$

$$D_{max} = (T + \Delta T) - [(R - \Delta R) + (I - \Delta I)] \tag{53}$$

$$D_{min} = (T - \Delta T) - [(R + \Delta R) + (I + \Delta I)] \tag{54}$$

Using Eq. 37 and Eq. 38 the range for the elastic deformation of the nozzle diameter can be calculated.

$$D_{max} = (3.11 + 0.0127) - [(2.010 - 0.686) + (0.92 - 0.0127)] = 0.8914mm$$

$$D_{min} = (3.11 - 0.0127) - [(2.010 + 0.0127) + (0.92 + 0.0127)] = 0.1419mm$$

The nozzle can elastically deform up to 0.89mm inside of the stopcock hole which illustrates that these tolerances are not extremely tight, and the manufacturing methods don't produce high tolerances. This interference fit can have profound variance in terms of the deformation and will still be able to withstand the force from a burette filled to 50mL.

V. Self-Assessment

The Reverse Engineering Report that I completed is rated 60/80. There was a lot of effort and careful thought that went into the completion of this report. The strengths of this report are the material analyses, the CAD models, the tolerance loops, the manufacturing analyses, and the assembly analysis. The CAD model that was developed is an extremely accurate representation of the burette that represent the dimensions and tolerances of the entire artifact. The material and assembly analyses consisted of comparing the theoretical values to the experimental values. Each part was physically evaluated to determine its material property and many manual assemblies were performed and timed. This comparison of the experimental values and theoretical values are in depth and illustrate how different the real world can be. The tolerance loops were created for each functional surface and more. They each depict what interfaces were being studied and the resulting tolerances which were calculated from using the tolerance loop analysis. The manufacturing analysis is the strongest section of the report for it goes into detail about each manufacturing method for each part along with the strengths and weaknesses of each method. It then compared the manufacturing methods and determined which one was the most cost effective and accurate. Then the analysis consisted of calculating different critical manufacturing values such as the force required to keep the nozzle on, and the maximum density of fluid before yielding occurs.

There are various weaknesses that are considerable throughout this report. The major weakness presented are the engineering analyses. This is because it was difficult to think in a creative sense about this generic object. Developing the physics behind some of the functions of the burette was difficult for me. While the engineering analyses I provided are adequate, there are plenty more engineering analyses that I needed to include to develop a full physical understanding of the burette. Some of the analyses are lacking proper derivations and calculations due to a lack of understanding and physical intuition. Another weakness in this report is the literature review. The literature review's goal is to provide history and inspiration of the current design. While I was able to find pertinent patents and information regarding this burette, I did not analyze it to its fullest extent. Trying to justify the functions and parts of the burette was difficult since I couldn't relate the history to the current iteration of the burette.

Overall, this is a strong report with many in depth analyses. The reason this report deserves a 60/80 rating is since the literature review and engineering analyses prevent it from being a perfect RER.

VI. CAD Model and Engineering Drawings

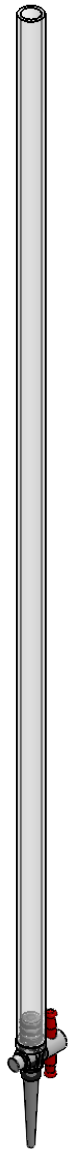

NOTES:
1. ALL DIMS IN MM
2. QTY: 1

TITLE: BURETTE ASSEMBLY			
DRAWN CYRIL MORAN			
DESIGNED CYRIL MORAN			
TOLERANCE UNLESS NOTED			
DIMENSION TYPE	PLACES IN DIMENSION 0.0	0.00	0.000
LOCATIONAL	±0.050	±0.020	±0.005
ANGULAR	±5	±2	±0.5

SIZE	DWG. NO.	REV
A	EML4501-A-001	A
SCALE: 1:4		SHEET 1 OF 5

5 4 3 2 1

ITEM NO.	PART NUMBER	DESCRIPTION	QTY.
1	EML4501-A-002	Burette Housing, Stopcock, and Nozzle Assembly	1
2	EML4501-A-003	Plug and Handle Assembly	1

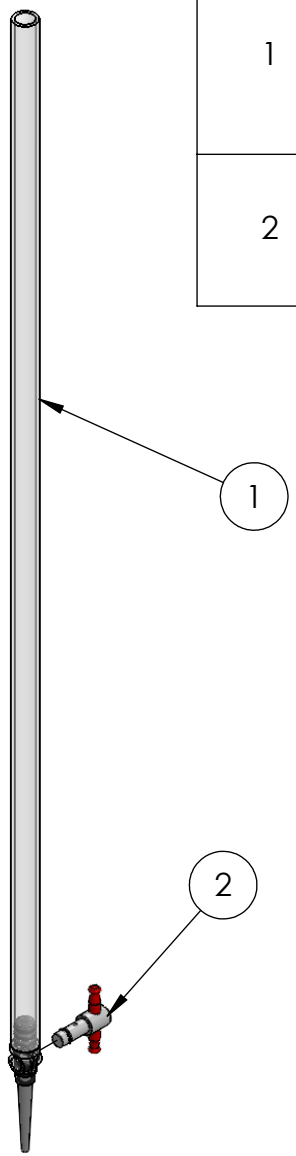

NOTES:
1. ALL DIMS IN MM
2. QTY: 1

TITLE: BURETTE ASSEMBLY			
DRAWN CYRIL MORAN			
DESIGNED CYRIL MORAN			
TOLERANCE UNLESS NOTED			
DIMENSION TYPE	PLACES IN DIMENSION 0.0	0.00	0.000
LOCATIONAL	±0.050	±0.020	±0.005
ANGULAR	±5	±2	±0.5
SIZE A	DWG. NO. EML4501-A-001		REV A
SCALE: 1:4			SHEET 2 OF 5

5 4 3 2 1

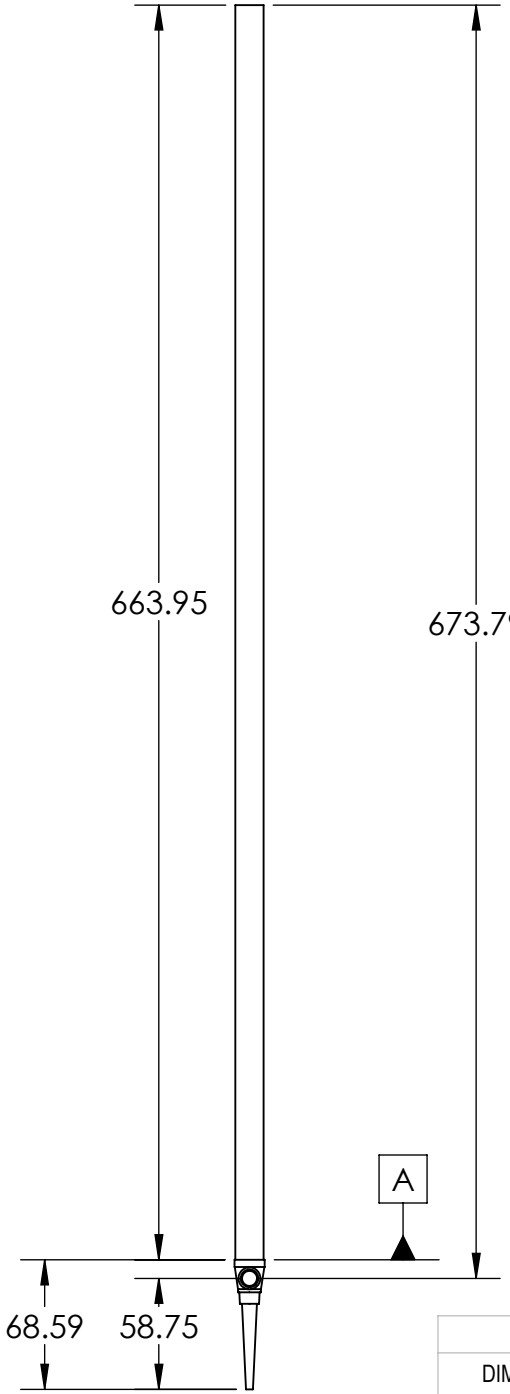

NOTES:
1. ALL DIMS IN MM
2. QTY: 1

TITLE:	BURETTE ASSEMBLY
DRAWN	CYRIL MORAN
DESIGNED	CYRIL MORAN

TOLERANCE UNLESS NOTED				SIZE	DWG. NO.	REV
DIMENSION TYPE	PLACES IN DIMENSION 0.0	0.00	0.000	A	EML4501-A-001	A
LOCATIONAL	±0.050	±0.020	±0.005			
ANGULAR	±5	±2	±0.5	SCALE: 1:4		SHEET 3 OF 5

5 4 3 2 1

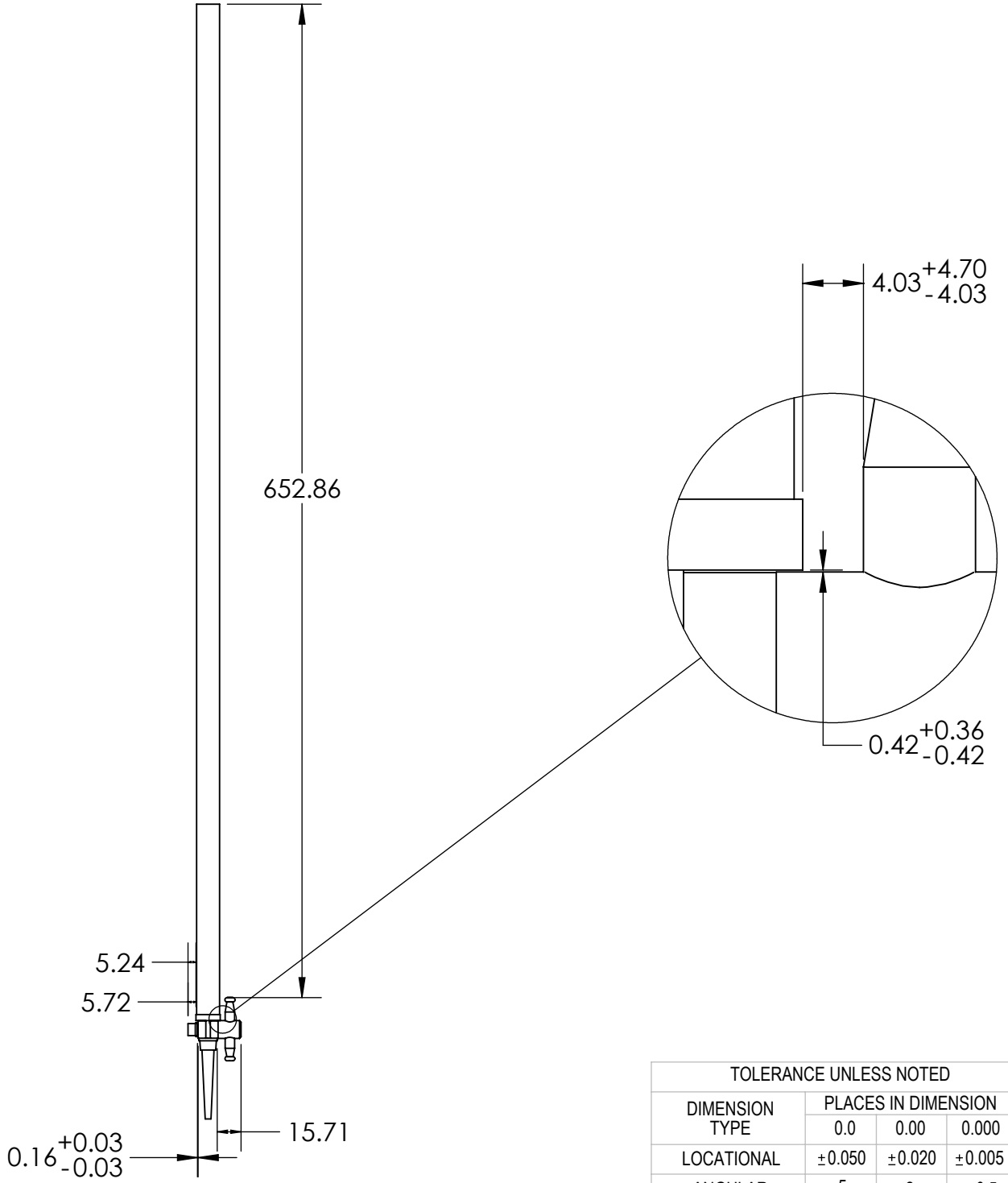

DETAIL B
SCALE 3 : 1

NOTES:
1. ALL DIMS IN MM
2. QTY: 1

TOLERANCE UNLESS NOTED				TITLE: BURETTE ASSEMBLY		
				DRAWN CYRIL MORAN		
				DESIGNED CYRIL MORAN		
DIMENSION TYPE	PLACES IN DIMENSION 0.0	0.00	0.000	SIZE A	DWG. NO. EML4501-A-001	REV A
LOCATIONAL	±0.050	±0.020	±0.005			
ANGULAR	±5	±2	±0.5	SCALE: 1:4		SHEET 4 OF 5

5 4 3 2 1

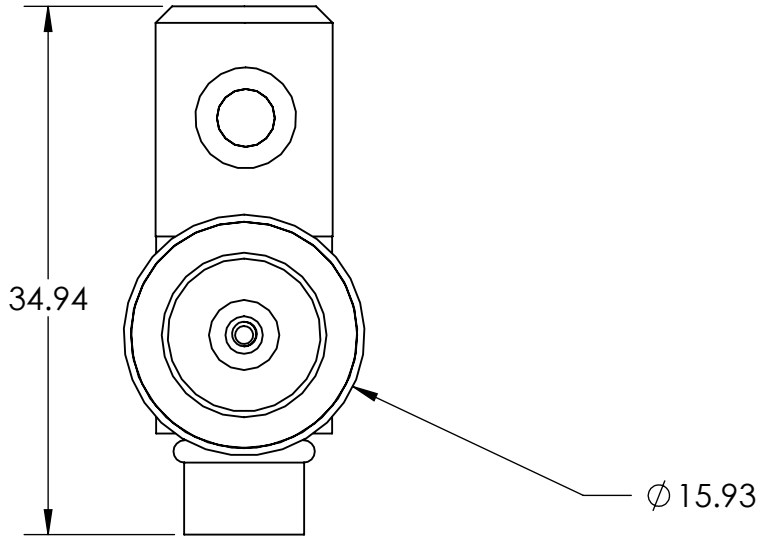

NOTES:
1. ALL DIMS IN MM
2. QTY: 1

TITLE: BURETTE ASSEMBLY						
DRAWN CYRIL MORAN						
DESIGNED CYRIL MORAN						
TOLERANCE UNLESS NOTED				SIZE	DWG. NO.	REV
DIMENSION TYPE	PLACES IN DIMENSION 0.0	0.00	0.000	A	EML4501-A-001	A
LOCATIONAL	±0.050	±0.020	±0.005			
ANGULAR	±5	±2	±0.5	SCALE: 1:0.5		SHEET 5 OF 5

5 4 3 2 1

NOTES:
1. ALL DIMS IN MM
2. QTY: 1

TITLE:	BURETTE HOUSING, NOZZLE, AND STOPCOCK ASSEMBLY		
DRAWN	CYRIL MORAN		
DESIGNED	CYRIL MORAN		

TOLERANCE UNLESS NOTED				SIZE	DWG. NO.	REV
DIMENSION TYPE	PLACES IN DIMENSION			A	EML4501-A-002	A
	0.0	0.00	0.000			
LOCATIONAL	±0.050	±0.020	±0.005			
ANGULAR	±5	±2	±0.5	SCALE: 1:4		SHEET 1 OF 4

5 4 3 2 1

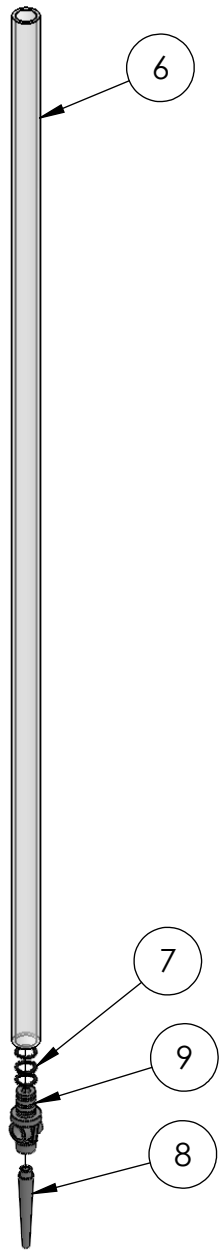

ITEM NO.	PART NUMBER	DESCRIPTION	QTY.
6	EML4501-004	Burette Housing	1
7	EML4501-005	Large O-Rings	3
8	EML4501-006	Nozzle	1
9	EML4501-007	Stopcock	1

NOTES:
1. ALL DIMS IN MM
2. QTY: 1

TITLE: BURETTE HOUSING, NOZZLE, AND STOPCOCK ASSEMBLY

DRAWN CYRIL MORAN

DESIGNED CYRIL MORAN

TOLERANCE UNLESS NOTED			
DIMENSION TYPE	PLACES IN DIMENSION		
	0.0	0.00	0.000
LOCATIONAL	±0.050	±0.020	±0.005
ANGULAR	±5	±2	±0.5

SIZE A | DWG. NO. EML4501-A-002 | REV A

SCALE: 1:4 | SHEET 2 OF 4

5 4 3 2 1

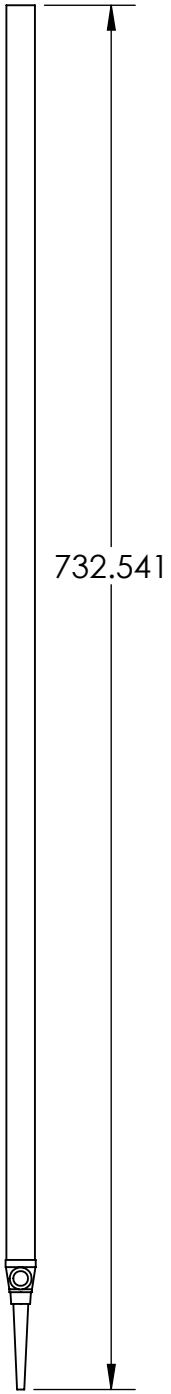

NOTES:
1. ALL DIMS IN MM
2. QTY: 1

TITLE:	BURETTE HOUSING, NOZZLE, AND STOPCOCK ASSEMBLY		
DRAWN	CYRIL MORAN		
DESIGNED	CYRIL MORAN		
TOLERANCE UNLESS NOTED			
DIMENSION TYPE	PLACES IN DIMENSION 0.0	0.00	0.000
LOCATIONAL	±0.050	±0.020	±0.005
ANGULAR	±5	±2	±0.5
SIZE: A	DWG. NO. EML4501-A-002		REV: A
SCALE: 1:4			SHEET 3 OF 4

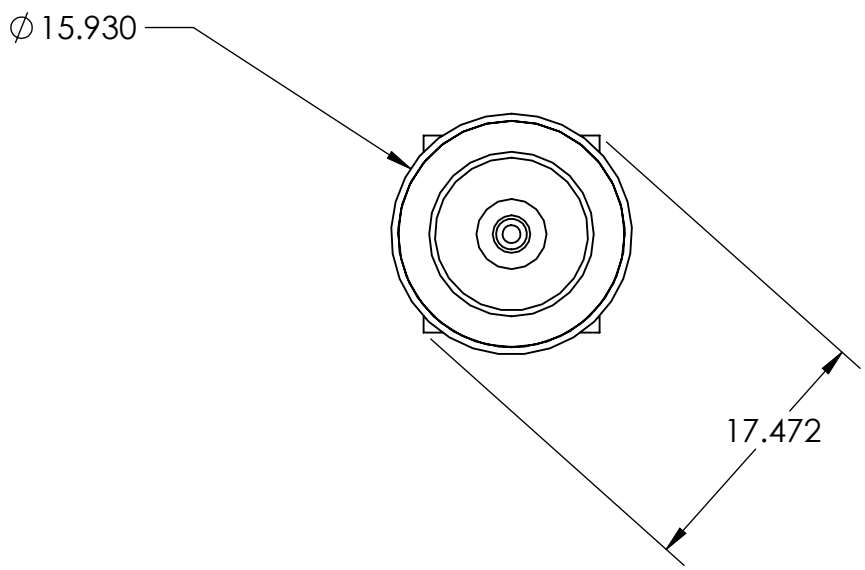

NOTES:
1. ALL DIMS IN MM
2. QTY: 1

TITLE: BURETTE HOUSING, NOZZLE, AND STOPCOCK ASSEMBLY			
DRAWN CYRIL MORAN			
DESIGNED CYRIL MORAN			
TOLERANCE UNLESS NOTED			
DIMENSION TYPE	PLACES IN DIMENSION		
	0.0	0.00	0.000
LOCATIONAL	±0.050	±0.020	±0.005
ANGULAR	±5	±2	±0.5
SIZE A	DWG. NO. EML4501-A-002		REV A
SCALE: 1:4			SHEET 4 OF 4

5 4 3 2 1

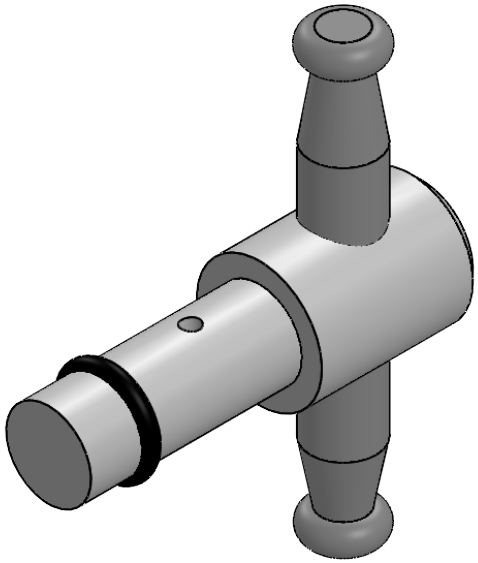

NOTES:
1. ALL DIMS IN MM
2. QTY: 1

				TITLE: PLUG AND HANDLE ASSEMBLY	
				DRAWN CYRIL MORAN	
TOLERANCE UNLESS NOTED				DESIGNED CYRIL MORAN	
DIMENSION TYPE	PLACES IN DIMENSION			SIZE	DWG. NO.	REV
	0.0	0.00	0.000	A	EML4501-A-003	A
LOCATIONAL	±0.050	±0.020	±0.005			
ANGULAR	±5	±2	±0.5	SCALE: 2:1		SHEET 1 OF 5

5 4 3 2 1

ITEM NO.	PART NUMBER	DESCRIPTION	QTY.
3	EML4501-001	Handle	1
4	EML4501-002	Stopcock Body	1
5	EML4501-003	Small O-ring	1

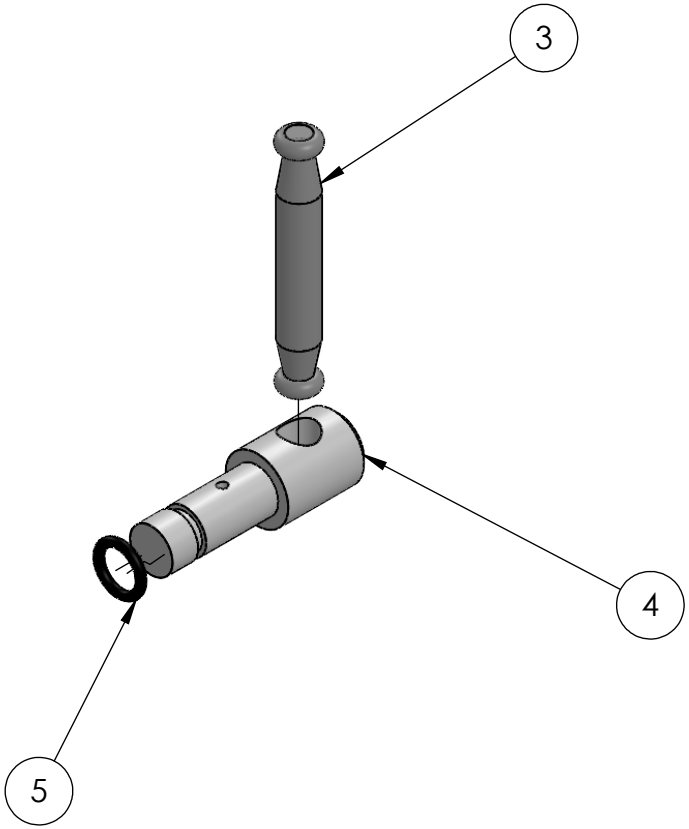

NOTES:
1. ALL DIMS IN MM
2. QTY: 1

TITLE:
PLUG AND HANDLE ASSEMBLY

DRAWN CYRIL MORAN
DESIGNED CYRIL MORAN

TOLERANCE UNLESS NOTED			
DIMENSION TYPE	PLACES IN DIMENSION		
	0.0	0.00	0.000
LOCATIONAL	±0.050	±0.020	±0.005
ANGULAR	±5	±2	±0.5

SIZE A | DWG. NO. EML4501-A-003 | REV A

SCALE: 1:1 | SHEET 2 OF 5

5 4 3 2 1

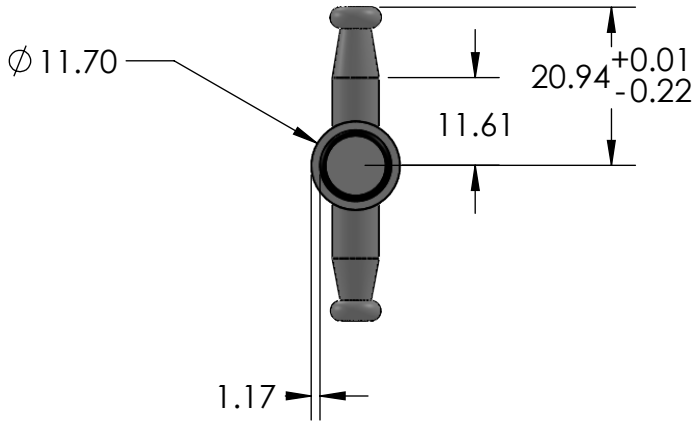

NOTES:
1. ALL DIMS IN MM
2. QTY: 1

TITLE: PLUG AND HANDLE ASSEMBLY						
DRAWN CYRIL MORAN						
TOLERANCE UNLESS NOTED	DESIGNED CYRIL MORAN					
DIMENSION TYPE	PLACES IN DIMENSION			SIZE	DWG. NO.	REV
	0.0	0.00	0.000	A	EML4501-A-003	A
LOCATIONAL	±0.050	±0.020	±0.005			
ANGULAR	±5	±2	±0.5	SCALE: 1:1		SHEET 3 OF 5

5 4 3 2 1

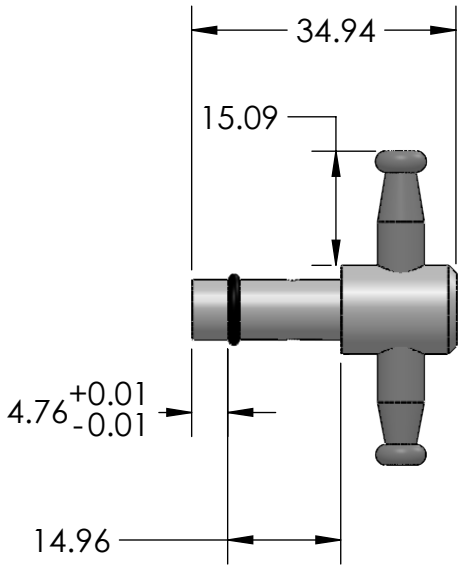

NOTES:
1. ALL DIMS IN MM
2. QTY: 1

TITLE: PLUG AND HANDLE ASSEMBLY						
DRAWN CYRIL MORAN						
TOLERANCE UNLESS NOTED	DESIGNED CYRIL MORAN					
DIMENSION TYPE	PLACES IN DIMENSION			SIZE	DWG. NO.	REV
	0.0	0.00	0.000	A	EML4501-A-003	A
LOCATIONAL	±0.050	±0.020	±0.005			
ANGULAR	±5	±2	±0.5	SCALE: 1:1		SHEET 4 OF 5

5 4 3 2 1

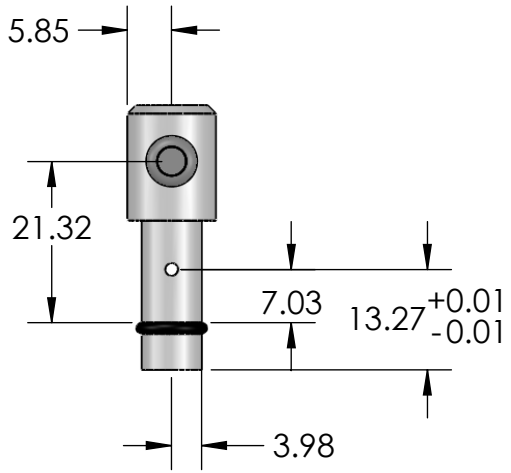

NOTES:
1. ALL DIMS IN MM
2. QTY: 1

TITLE: PLUG AND HANDLE ASSEMBLY						
DRAWN CYRIL MORAN						
TOLERANCE UNLESS NOTED	DESIGNED CYRIL MORAN					
DIMENSION TYPE	PLACES IN DIMENSION			SIZE	DWG. NO.	REV
	0.0	0.00	0.000	A	EML4501-A-003	A
LOCATIONAL	±0.050	±0.020	±0.005			
ANGULAR	±5	±2	±0.5	SCALE: 1:1		SHEET 5 OF 5

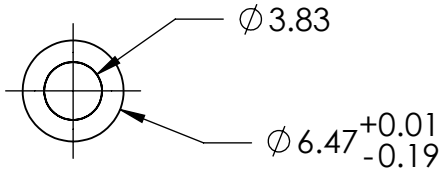

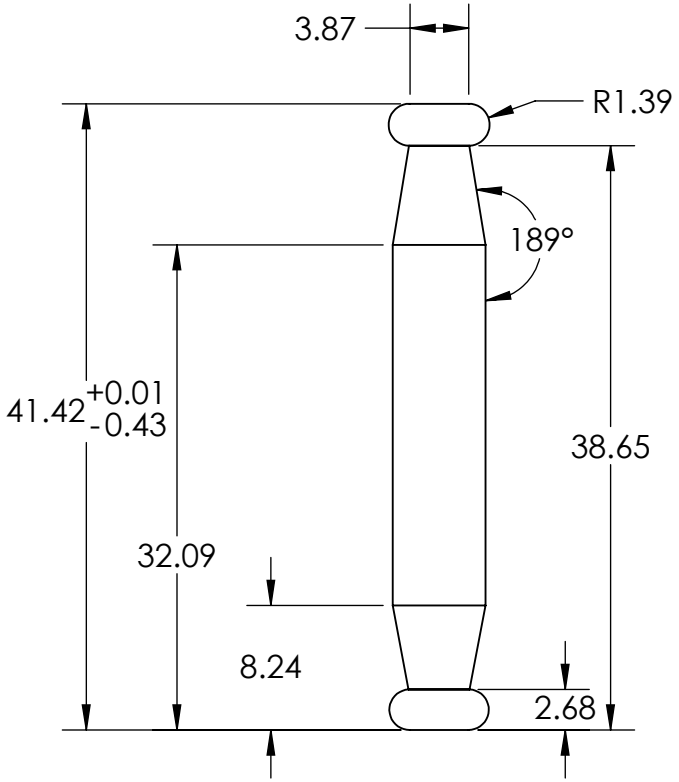

NOTES:
1. ALL DIMS IN MM
2. QTY: 1
3. MAT'L: PE

TOLERANCE UNLESS NOTED				TITLE: HANDLE		
OPERATION	PLACES IN DIMENSION					
	0.0	0.00	0.000	DRAWN	CYRIL MORAN	
MACHINING	±0.050	±0.020	±0.005	DESIGNED	CYRIL MORAN	
INJECTION MOLDING	±0.1	±0.0127		SIZE A	DWG. NO. EML4501-001	REV A
WELDING	±0.1	±0.060				
ANGULAR DIMS	±5	±2	±0.5	SCALE: 2:1		SHEET 1 OF 1

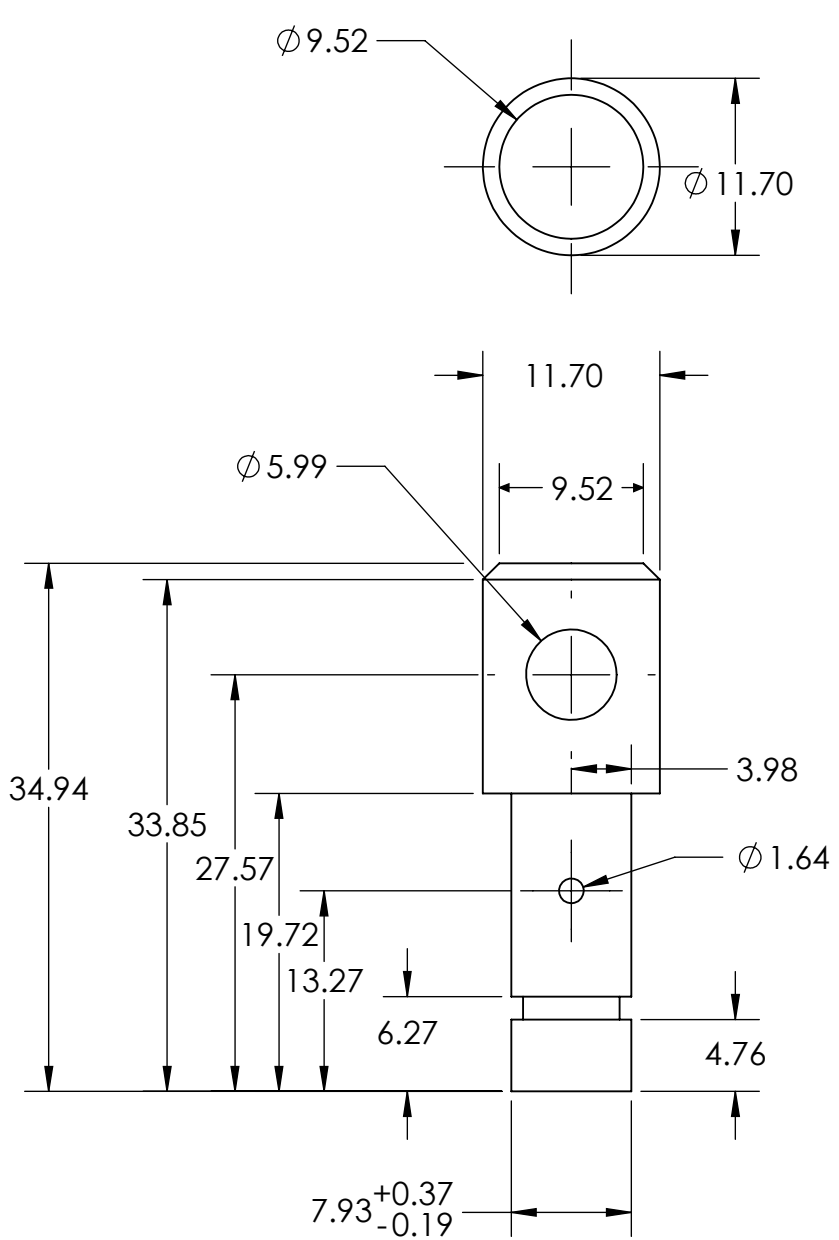

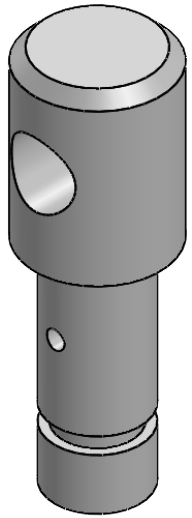

NOTES:
1. ALL DIMS IN MM
2. QTY: 1
3. MAT'L: PTFE

TOLERANCE UNLESS NOTED				TITLE: STOPCOCK BODY		
OPERATION	PLACES IN DIMENSION					
	0.0	0.00	0.000	DRAWN	CYRIL MORAN	
MACHINING	±0.050	±0.020	±0.005	DESIGNED	CYRIL MORAN	
PTFE Compression Molding	±0.1	±0.0127		SIZE	DWG. NO.	REV
WELDING	±0.1	±0.060		A	EML4501-002	A
ANGULAR DIMS	±5	±2	±0.5	SCALE: 2:1		SHEET 1 OF 1

5 4 3 2 1

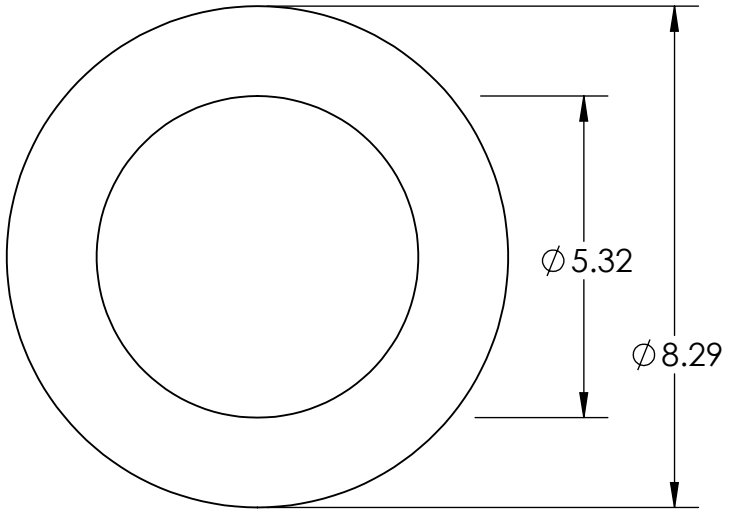

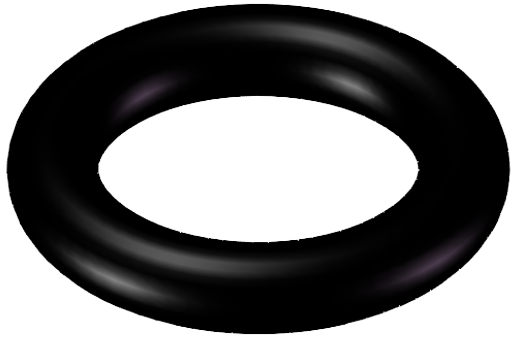

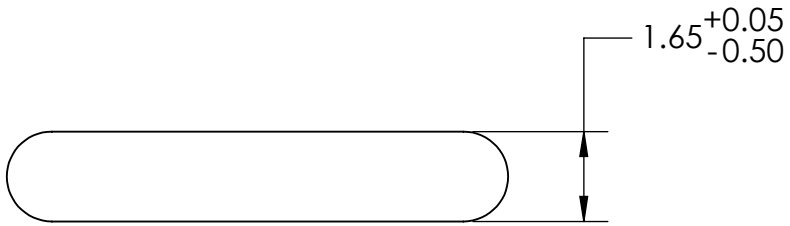

NOTES:
1. ALL DIMS IN MM
2. QTY: 1
3. MAT'L: STYRENE

TOLERANCE UNLESS NOTED				TITLE: SMALL O-RING		
OPERATION	PLACES IN DIMENSION					
	0.0	0.00	0.000	DRAWN	CYRIL MORAN	
MACHINING	±0.050	±0.020	±0.005	DESIGNED	CYRIL MORAN	
COMPRESSION MOLDING	±0.15	±0.102		SIZE	DWG. NO.	REV
WELDING	±0.1	±0.060		A	EML4501-003	A
ANGULAR DIMS	±5	±2	±0.5	SCALE: 8:1		SHEET 1 OF 1

5 4 3 2 1

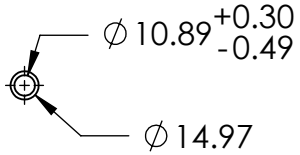

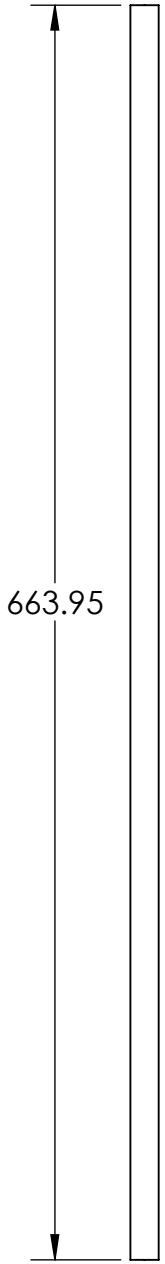

NOTES:
1. ALL DIMS IN MM
2. QTY: 1
3. MAT'L: ACRYLIC

TOLERANCE UNLESS NOTED				TITLE: BURETTE HOUSING		
OPERATION	PLACES IN DIMENSION					
	0.0	0.00	0.000	DRAWN	CYRIL MORAN	
MACHINING	±0.050	±0.020	±0.005	DESIGNED	CYRIL MORAN	
THERMOFORMING	±0.31	±0.3		SIZE	DWG. NO.	REV
WELDING	±0.1	±0.060		A	EML4501-004	A
ANGULAR DIMS	±5	±2	±0.5	SCALE: 4		SHEET 1 OF 1

5 4 3 2 1

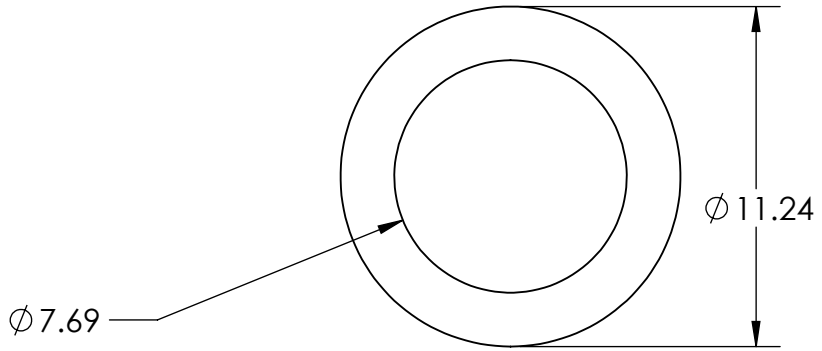

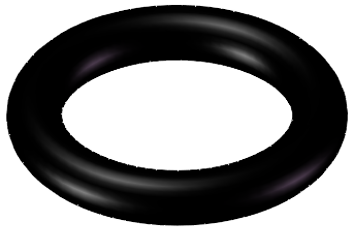

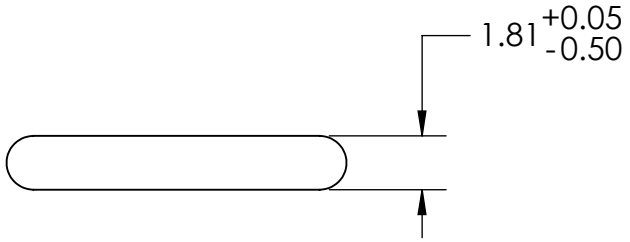

NOTES:
1. ALL DIMS IN MM
2. QTY: 3
3. MAT'L: STYRENE

TOLERANCE UNLESS NOTED				TITLE: LARGE O-RINGS		
OPERATION	PLACES IN DIMENSION					
	0.0	0.00	0.000	DRAWN	CYRIL MORAN	
MACHINING	±0.050	±0.020	±0.005	DESIGNED	CYRIL MORAN	
COMPRESSION MOLDING	±0.15	±0.102		SIZE	DWG. NO.	REV
WELDING	±0.1	±0.060		A	EML4501-005	A
ANGULAR DIMS	±5	±2	±0.5	SCALE: 4:1		SHEET 1 OF 1

5 4 3 2 1

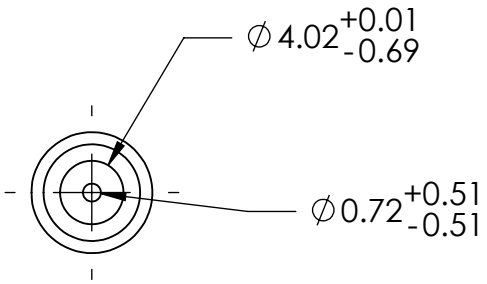

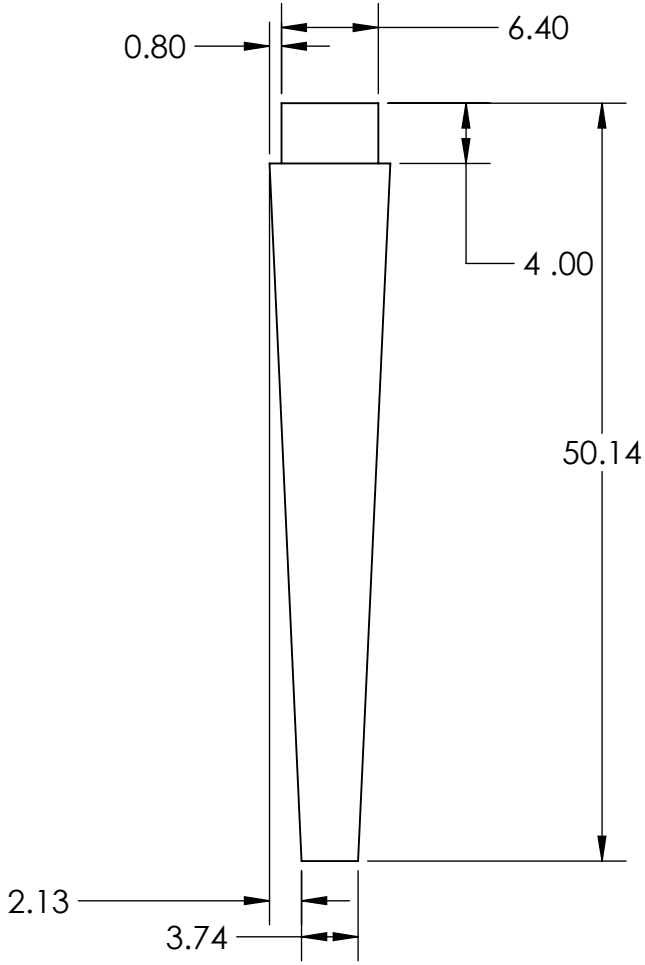

NOTES:
1. ALL DIMS IN INCHES
2. QTY: 1
3. MAT'L: PP

TOLERANCE UNLESS NOTED				TITLE: NOZZLE		
OPERATION	PLACES IN DIMENSION					
	0.0	0.00	0.000	DRAWN	CYRIL MORAN	
MACHINING	±0.050	±0.020	±0.005	DESIGNED	CYRIL MORAN	
INJECTION MOLDING	±0.1	±0.0127		SIZE	DWG. NO.	REV
WELDING	±0.1	±0.060		A	EML4501-006	A
ANGULAR DIMS	±5	±2	±0.5	SCALE: 2:1		SHEET 1 OF 1

5 4 3 2 1

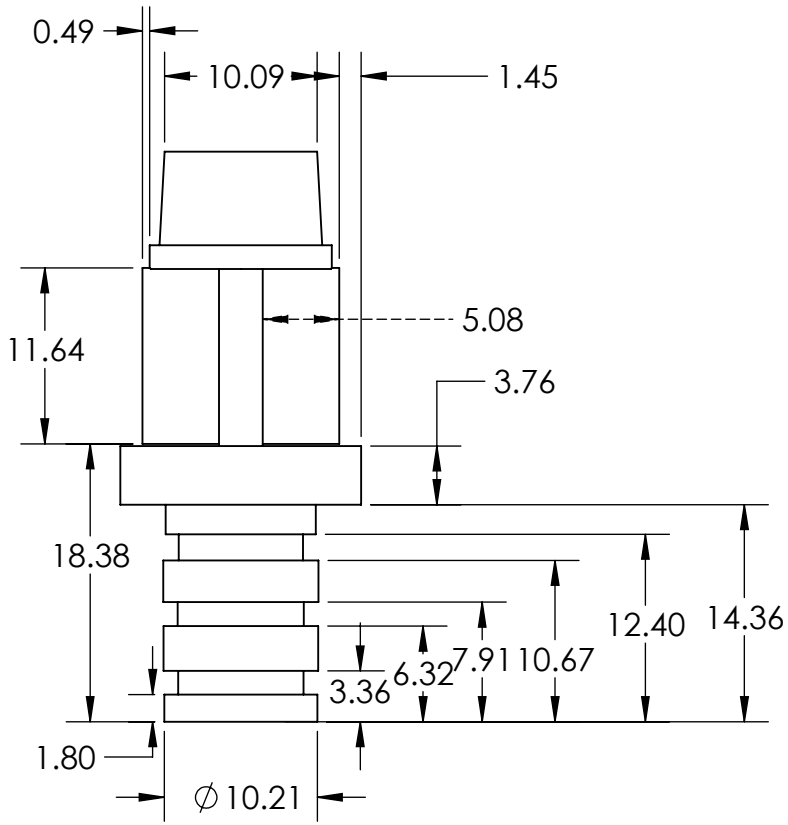

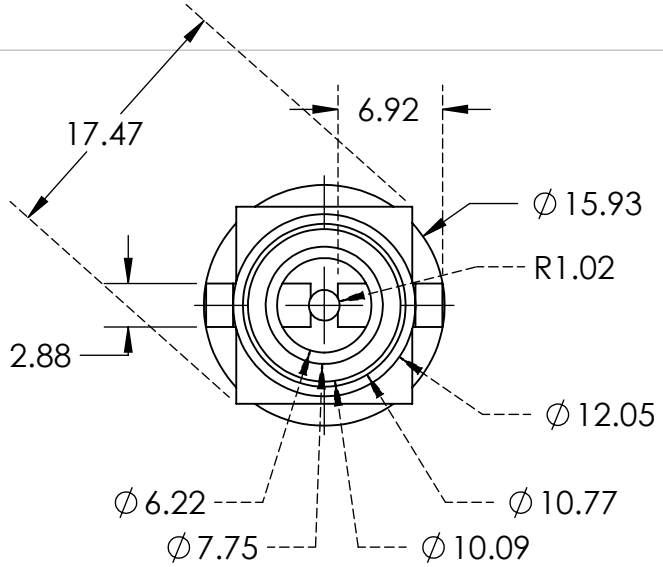

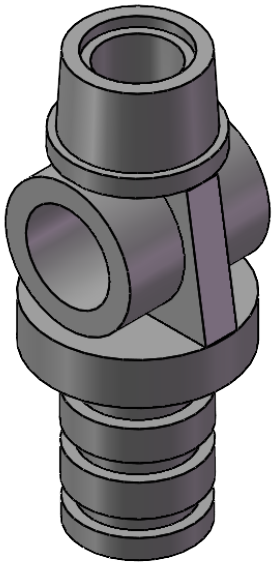

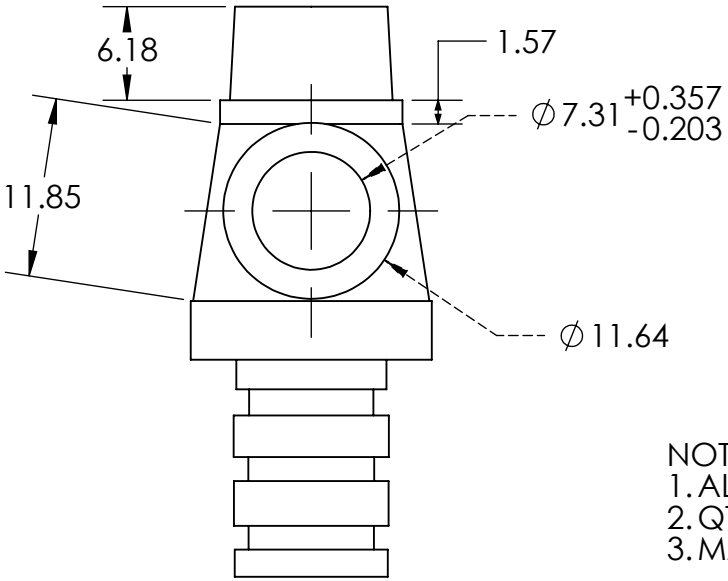

NOTES:
1. ALL DIMS IN MM
2. QTY: 1
3. MAT'L: PE

TOLERANCE UNLESS NOTED				TITLE: STOPCOCK	
OPERATION	PLACES IN DIMENSION				
	0.0	0.00	0.000	DRAWN	CYRIL MORAN
MACHINING	±0.050	±0.020	±0.005	DESIGNED	CYRIL MORAN
INJECTION MOLDING	±0.1	±0.0127		SIZE: A	DWG. NO.: EML4501-007
WELDING	±0.1	±0.060			REV: A
ANGULAR DIMS	±5	±2	±0.5	SCALE: 2:1	SHEET 1 OF 1

5 4 3 2 1

References

[1]Gramann, Paul, Antoine C. Rios and Bruce A. Davis. “FAILURE OF THERMOSET VERSUS THERMOPLASTIC MATERIALS.” (2005).

[2] “Weight of a hand,” What Things Weigh Available: https://whatthingsweigh.com/how-much-does-a-hand-weigh/.

[3] An, Yongki & Joo, Byung & Chung, Dong-Teak & Choi, Se. (2014). Finite Element Simulation of Brittle Fracture of Bulletproof Glass System. Journal of Mechanical Science and Technology. 28. 10.1007/s12206-013-0943-8.

[4] Kodys, A. & Murray, Robert & Cassady, Leonard & Choueiri, Edgar. (2006). An Inverted-Pendulum Thrust Stand for High-Power Electric Thrusters. 10.2514/6.2006-4821.

[5] Thomas, S., “How to design for stiffness using a geometric approach,” *Fictiv* Available: https://www.fictiv.com/articles/how-to-design-for-stiffness-using-a-geometric-approach.

[6] O’Sullivan LW, Gallwey TJ. “Forearm Torque Strength and Endurance for Elbow and Forearm Angles,” *Proceedings of the Human Factors and Ergonomics Society Annual Meeting*. 2001;45(14):1128-1132. doi:10.1177/154193120104501430

[7] “Injection molding tolerances: Best practices: Resources: Fast radius,” *Injection Molding Tolerances: Best Practices | Resource Fast Radius* Available: https://www.fastradius.com/resources/injection-molding-tolerances-best-practices/#:~:text=Injection%20molds%20are%20typically%20CNC,001%20inches.

[8] Dunbeck, J. T., and Hanf, W. K., “Stopcock,” , June 12, 1962.

[9] Hudson, J., The history of Chemistry, London: MacMillan, 1994.

[10] Traum, M. “Boothroyd & Dewhurst technique, “ University of Florida, Mechanical Design 2, 2022.

[11] Shah, V., “Plastics and Elastomers Identification Chart,”Consultek, Brea, CA

[12] Traum, M. “Solder Iron Touching Handle, “ University of Florida, Mechanical Design 2, 2022.

[13] Traum, M. “Solder Iron Touching Nozzle, “ University of Florida, Mechanical Design 2, 2022.

[14] Traum, M. “Solder Iron Touching Stopcock, “ University of Florida, Mechanical Design 2, 2022.

[15] Traum, M. “Solder Iron Touching Burette Housing, “ University of Florida, Mechanical Design 2, 2022.

[16] “Supertek Catalog,” Supertek Scientific, LLC, 2020 [online database], URL: https://static1.squarespace.com/static/5e222e24f9a4f85b4d689d2c/t/5e7baa37173f4c14e4ec0754/1585162838582/2020+Supertek+Catalog+v3.25_compressed.pdf [retrieved 24 May 2022].

[17] “What are plastic injection moulding advantages and disadvantages ?,” *Plastic Injection Moulding Advantages & Disadvantages* Available: https://www.toolcraft.co.uk/plastic-injection-moulding/advice/advice-plastic-injection-moulding-advantages-disadvantages.htm.

[18] Engineering Department | Pacific Research Labsinfo@pacific-research.comPRL’s engineers have dozens of manufacturing options available to help you solve any challenge facing your product: CNC machining, “The advantages and disadvantages of thermoforming,” *Pacific Research* Available: https://www.pacific-research.com/the-advantages-and-disadvantages-of-thermoforming-prl/.

[19]*, N., “Advantages and disadvantages of compression molding - liquid injection molding, die cutting and rubber molding: Elastomer Technologies,” *Liquid Injection Molding, Die Cutting and Rubber Molding | Elastomer Technologies* Available: https://www.etiroltec.com/advantages-disadvantages-compression-molding/.

[20] “Materials used - PTFE,” Micromold Available: https://micromold.com/materials_ptfe.html#:~:text=Since%20PTFE%20will%20not%20flow,analogous%20to%20sintered%20metal%20processing.

[21] “Standard tolerance chart for rubber molded parts: MN rubber,” Minnesota Rubber & Plastics Available: https://www.mnrubber.com/tools-resources/design-guide/designing-rubber-components/standard-tolerance-chart/.

[22] “Thermoforming Tolerances: Design Guide chapter 5,” Ray Products Available: https://www.rayplastics.com/thermoforming-tolerances-design-guide-chapter-5/.

[23] Mohammed, Taib., “*Study of the effect of the shape of the miniplate on the stability of mandibular symphyseal fracture using finite element analysis*.” Egyptian Journal of Oral and Maxillofacial Surgery., 2018, 9. 10.21608/OMX.2018.3584.1002.

[24] Admin, “Mercury element (hg) [liquid metal] - density, boiling point, Properties & uses of Mercury element,” *Mercury* Available: https://byjus.com/chemistry/mercury/.